LA-UR-16-25649
Approved for public release; distribution is unlimited.

Title: Deep Boreholes Seals Subjected to High P, T conditions – Preliminary Experimental Studies

Author(s): Caporuscio, Florie Andre
Norskog, Katherine Elizabeth
Maner, James Lavada

Intended for: Report

Issued: 2017-01-18 (rev.1)

Deep Boreholes Seals Subjected to High P, T conditions – Preliminary Experimental Studies

Fuel Cycle Technology

Prepared for
U.S. Department of Energy
Campaign or Program
Caporuscio, F.A.[1],
Norskog, K.E[1],
And Maner, J[2].
[1]Los Alamos National Laboratory
[2]University of Oklahoma

July 29, 2016
FCRD-UFD-2016-000615
'LA-UR-16-25649

CONTENTS

FIGURES

TABLES

Acronyms

DB – Deep Borehole experiment
DBS – Deep Borehole Small experiment
EBS – Engineered Barrier System
EMP – Electron Microprobe
EPA – Environmental Protection Agency
EDX – Energy dispersive X-ray
LANL – Los Alamos National Lab
QXRD – Quantitative X-ray Diffraction
RIR – Reference Intensity Ratio
SEM – Scanning Electron Microscope
THCM – Thermal-Hydrological-Chemical-Mechanical
TMC Thermal-Mechanical-Chemical
XRD- X-ray diffraction

Deep Boreholes Seals Subjected To High P, T Conditions – Preliminary Experimental Studies

1. Objective

The objective of this planned experimental work is to evaluate physio-chemical processes for 'seal' components and materials relevant to deep borehole disposal. These evaluations will encompass multi-laboratory efforts for the development of seals concepts and application of Thermal-Mechanical-Chemical (TMC) modeling work to assess barrier material interactions with subsurface fluids, their stability at high temperatures, and the implications of these processes to the evaluation of thermal limits. Deep borehole experimental work will constrain the Pressure, Temperature (P, T) conditions which "seal" material will experience in deep borehole crystalline rock repositories. The rocks of interest to this study include the silicic (granitic gneiss) end members. The experiments will systematically add components to capture discrete changes in both water and EBS component chemistries.

2. Introduction

Evaluations of deep borehole disposal have been presented from several countries in the past (O'Brien et al. 1979; Woodward and Clyde Consultants 1983; Juhlin and Sandstedt 1989; Heiken et al. 1996; Nirex 2004; Anderson 2004; Gibb et al. 2008a). More recently Sandia National Laboratory has embarked on a review study (Brady, et.al., 2009) designing a reference case (Arnold, et.al., 2011), performing THCM modeling for deep borehole disposal system (Arnold and Hadgu, 2013) and creating guidelines for a demonstration project site selection, seals design, and R&D needs (Arnold, et.al. 2013).

The document "Sealing deep site investigation boreholes: Phase 1 report" produced by Amec (2014) for the British government, represents a high level summary document concerning seals. Although broad in scope, this has somewhat limited applications to the US program. First, repository conditions in the US will be more extreme than most scenarios developed in the report. Second, the rock types for Briton are more disparate than the crystalline rock slated for the US mission. There are some significant points to be taken from the document.

- Bentonite will be the main seal component

- Interaction with support seals (concrete) may be problematic due to high pH generated and subsequent smectite destabilization.
- Smectites in seals may react substantially different from EBS because of lower volumes and significantly higher surface area.

- **Experiments need to be performed in the correct P,T, space for deep boreholes and capture the correct chemical domains**
- Ability to scale up is critical
- **No mention of bentonite to capture Cs, Sr if released from capsules. These experiments will be invaluable to the US program.**
- The document set forth both a modeling system (different from US) and subsequent up flow of data to a PA.
- The document also has a flow chart that the US Deep Boreholes program may be able to use as a starting template

Arnold, et.al. (2013) stated in their Section 3.2 :Review of Bentonite and Cement Seals Stability
"Bentonite volume is reduced by high ionic strength and/or the introduction of divalent cations, such as Ca+2, Mg+2, and Fe+2 (produced during the anoxic corrosion of steel casing). Brines at the bottom of the borehole are expected to have high ionic strengths and appreciable levels of divalent cations; fluids above the waste emplacement zone will be more dilute; bentonites near cement may be subjected to high Ca+2 levels; and bentonites near degrading steel may see high Fe+2 and Ni+2 concentrations. Temperatures in the upper reaches of the borehole will be 25 – 75oC; they may approach 150oC at depth. Hydrostatic pressures will approach 115 - 340 bar (11.5 - 34.0 MPa) at depth. High temperatures should accelerate reactions, but may also shift the mineral equilibria that influence dissolved concentrations. For example, higher temperatures will favor dissolution of feldspars, thereby increasing dissolved Na+, K+, and SiO2 levels, and possibly prompting the formation of new clay minerals.
Batch bentonite equilibration experiments will be done at 50 and 150°C as a function of salinity and divalent cation concentration to measure volume and mineralogy changes as a function of temperature. Reactants will be loaded into a flexible gold bag and fixed into a 500 mL Gasket Confined Closure reactor (Seyfried et al. 1987). Experiments will be pressurized to 150 - 160 bar (15.0 – 16.0 MPa) and heated to follow two different temperature profiles: (1) 120°C for 2 weeks, 220°C for 2 weeks, and then 300 °C for 1 week and (2) isothermal at 300 °C for 6 weeks. Reaction liquids extracted during the experiments will be analyzed to investigate the aqueous geochemical evolution in relationship to mineralogical alterations. Geochemical modeling will be used to develop a methodology for predicting limits of bentonite reactivity as a function of depth, time, and proximity to degrading steels and cements."

Since Arnold et. al. (2013), discussions with Sandia personnel have formulated a much more discrete starting experimental system. Initial experiments will not contain cement or cement reaction. Experiments in the **clay-water system** will evaluate interactions among components, including: mineral phase stability, and thermal limits. Based on engineered barrier studies, experimental investigations will move forward with two focusses. **First**, evaluation of interaction

between “seal” materials under fluid-saturated conditions over long-term (i.e., two-month) experiments; which reproduces the bottom of the seal plug at 3 km of a deep borehole repository. **Second**, perform experiments to determine the stability of zeolite minerals (analcime-wairakite$_{ss}$) under cesium contamination if repository fails at 5 km depth (Figure 1). Both sets of experiments are critically important for understanding mineral paragenesis (zeolites and/or clay transformations) associated with “seals” at elevated temperatures.

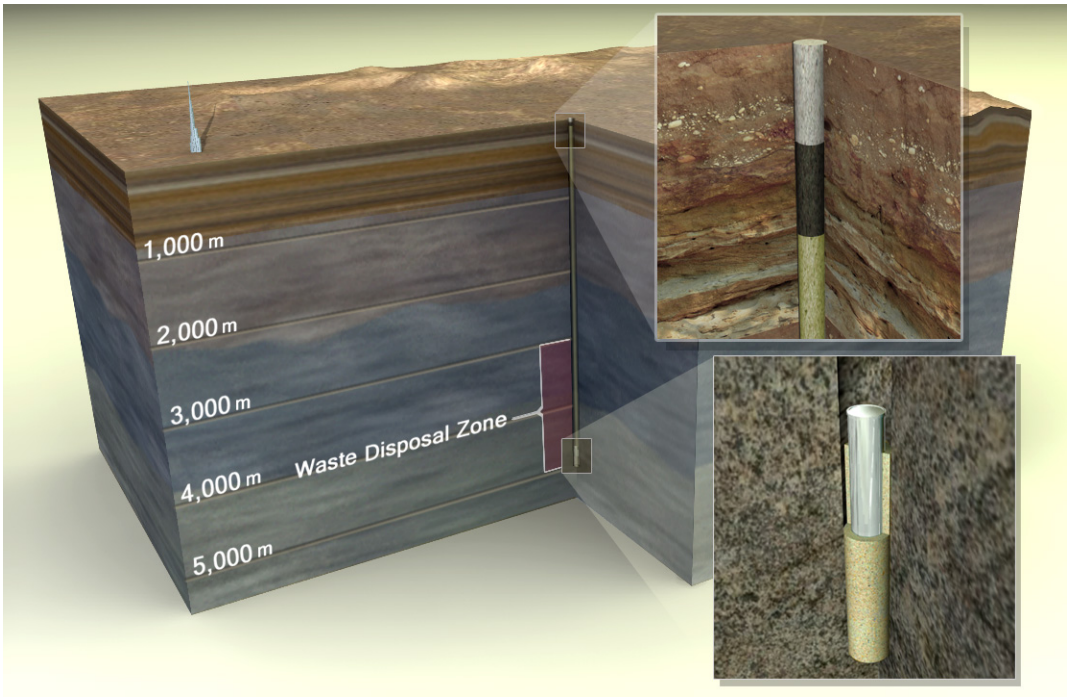

Figure 1. 3D schematic of proposed deep borehole. Lower right image shows canister at bottom of borehole.

2.1 Previous Engineered Barrier System experimental work

Caporuscio et al. (2015) provides a comprehensive overview of experiments conducted at LANL for the EBS program. Experiments were conducted at temperatures between 100°C and 300°C for 1 to 2 months at a pressure of 150-160 bars with a fluid:solid ratio of 9:1. The more important conclusions to note here are (1) the corrosion rates of different metals under the experimental conditions, (2) stability of smectite at high temperature/ pressure and (3) the formation of zeolites at the expense of bentonite clay materials (clinoptilolite / glass).

- Runs containing Fe metal (both as a 'container' material and an oxygen fugacity buffer) produced Fe-phyllosilicates (Fe-saponite and stilpnomelane) at the clay metal interface. Corrosion rates for the metals varied from 9-44 µm for 6 week experiments.

- Smectite did not evolve to illite during the course of the experiments. Illite or illite/smectite mixed-layer formation was significantly retarded in the closed system due to a limited K+ supply along with high Na+ and $SiO_{2(aq)}$ concentrations (Cheshire, et. al, 2014).

- The reaction of bentonite (sodic) clay and opalinus (calcic) clay with brine solution produced a zeolites whose compositions lie between analcime (An: $NaAlSi_2O_6*H_2O$) and wairakite (Wrk: $CaAl_2Si_4O_{12}*2H_2O$). In experiments using bentonite clay only, zeolites with a composition of $An_{85}Wrk_{15}$ (±10 mole %) formed. When the opalinus clay was used, zeolites with a composition of $An_{22}Wrk_{78}$ formed. Intermediate compositions comprised of a mixture of clays produced zeolites intermediate between the other experiments (i.e. $An_{64}Wrk_{36}$). This is the first reported synthesis of zeolites along the analcime-wairakite solid solution.

3. Methods / Materials

Our laboratory has two hydrothermal systems available: 1) rocking autoclaves (Figures 2-4) and 2) cold seal reaction vessels (Figures 5-7). The rocking autoclaves are capable of temperatures of 400 ^oC and 600 bar, while the cold seal reactors are capable of reaching 800°C and 2000 bars. Mid-experiment gaseous and aqueous samples can be obtained from the rocking autoclaves, however fluid sampling cannot be obtained mid-experiment with the cold seal vessels.

Figure 2) Rocking autoclave images

Figure 3) Gold reaction cells:

Top: 120cc cell

Bottom: 240cc cell with cap, thrust ring, and head disassembled

Figure 4) Left: HIP (thrust ring seal type) pressure vessel, for 400c/600bar furnaces
Right: AE (bridgeman seal type) pressure vessel, for 600c/1.5kBar furnaces
(vessel is ~24” tall)

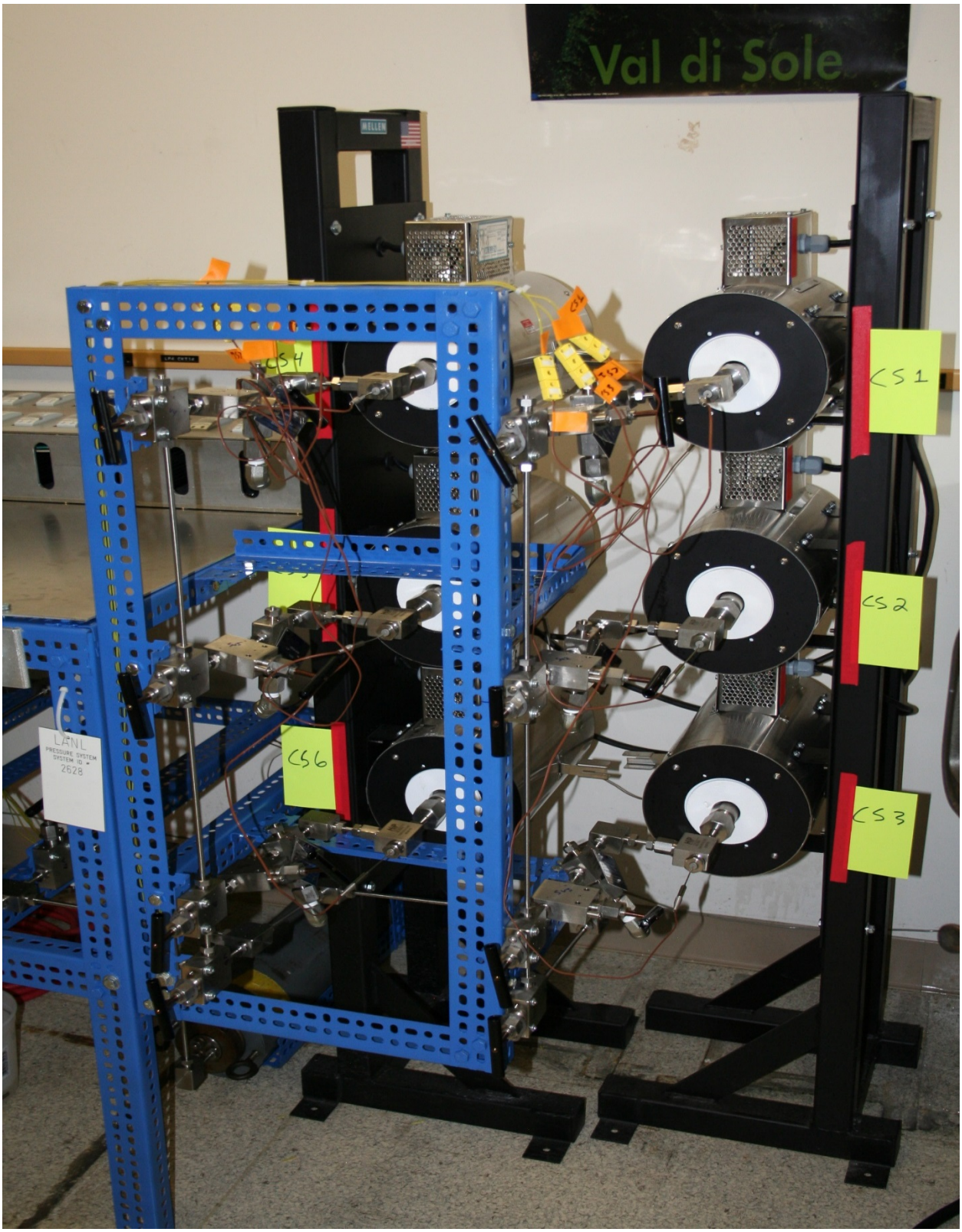

Figure 5) Cold Seal reaction system. Upper temperature /pressure limits are 800 ºC, and 2.5 Kb.

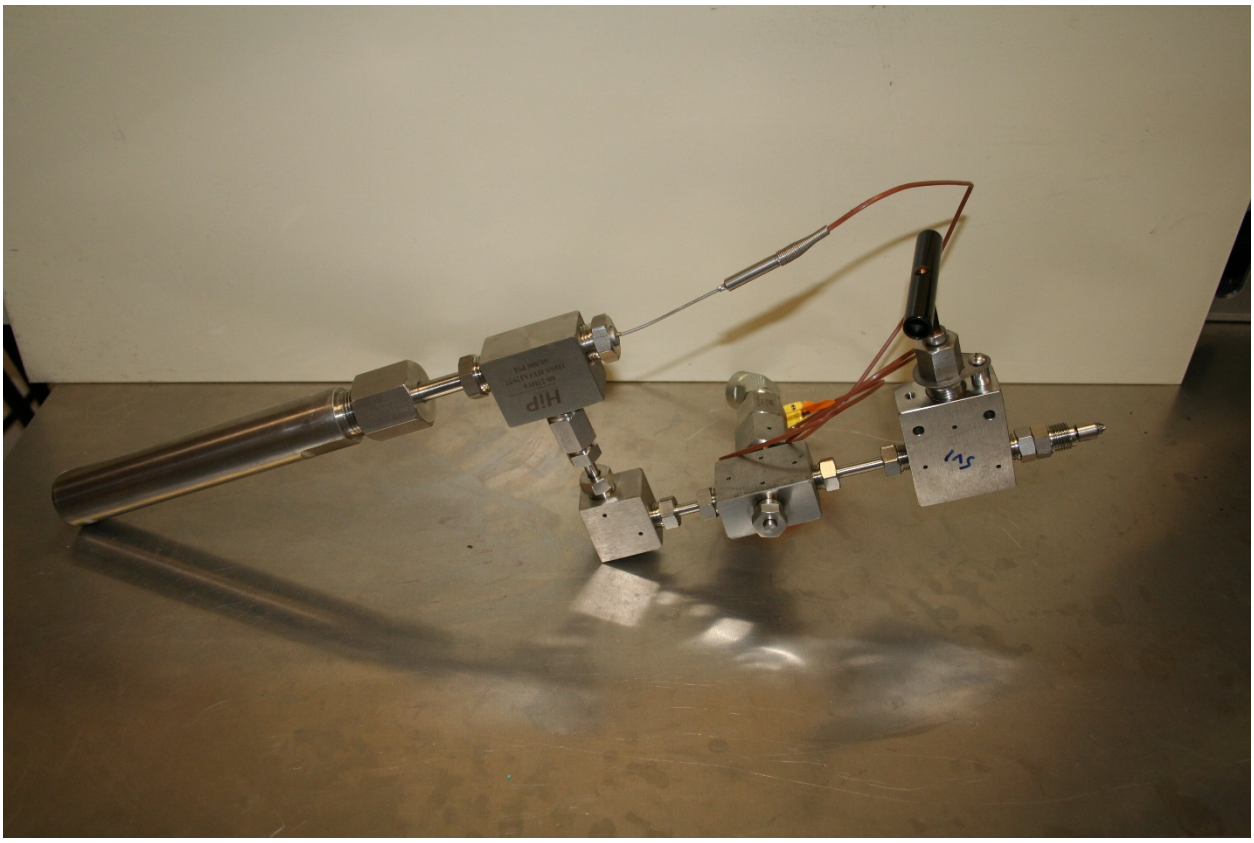

Figure 6) Hard plumbed cold seal reaction vessel system. Reaction vessel is at far left.

Figure 7) Cold seal system gold reaction capsules, approximately 2.5 cm in length.

For the first year program, the objectives are to obtain simple system proof of principle results. The first experimental design is to mimic the base of the seals plug at 3 kilometer depth. Two experiments are planned, with no metals involved. The second was to replicate the early failure of a canister due to borehole collapse at 5 km depth Materials /parameters for the first year campaign are:

EXPERIMENT 1) – BASE OF SEALS
Temperature: 150 ^{o}C
Pressure: 300 bar
Time: 8 weeks
Seal material: unprocessed bentonite clay from Colony, WY.
Brine: NaCl, CaCl, 2 molal
Rocking Autoclaves: – 200 ml capacity

EXPERIMENT 2) – BASE OF HOLE – CANISTER RUPTURE DUE TO HOLE COLLAPSE

Temperature: 400 ^{o}C
Pressure: 1000 bar
Time: 2 weeks
Seal material: unprocessed bentonite clay from Colony, WY.
Brine: NaCl, CaCl, Cs/Ca/NaCl 2 molal
Cold Seal Gold Capsule – 4 ml capacity

Fluid samples will be drawn weekly and analyzed for major cations / anions via mass spectrometer. Experimental products (as Polished epoxied grain thin sections) will be inspected and preliminarily characterized by transmitted and reflected light microscopy. Samples will then be analyzed with an electron microprobe (at the University of Oklahoma) to determine their chemical compositions. Loose products can be ground to a fine powder and analyzed via X-ray diffraction and SEM at LANL.

3.1 Experimental Setup

The bentonite used in this experimental work is mined from a reducing horizon in Colony, Wyoming. The bentonite was pulverized and sieved to < 3 mm and used with a free moisture of ~15.5 wt. %. The synthetic groundwater solutions were simple brines (NaCl, CaCl, or Cs/Ca/NaCl). The groundwater solution was prepared using reagent grade materials dissolved in double deionized water. NaOH and HCl were added to adjust the initial solution pH. This

solution was then filtered through a 0.45 μm filter and sparged with He before each experiment. The salt solution was added at 9:1 water: bentonite ratio. Initial components for all experiments have been summarized in Table 3.The redox conditions for each system were buffered using a 1:1 mixture (by mass) of Fe_3O_4 and Fe° added at 0.07 wt. % of the bentonite mass.
For the base of seal experiments (3 km depth) reactants were loaded into a flexible gold bag and fixed into a 500 mL Gasket Confined Closure reactor (Seyfried et al. 1987). Experiments were pressurized to 300 bar and were heated at 150 °C for 8 weeks. Reaction liquids were extracted during the experiments and analyzed to investigate the aqueous geochemical evolution in relationship to mineralogical alterations. The sampled reaction liquids were split three-ways producing aliquots for unfiltered anion, unfiltered cation, and filtered (0.45 μm syringe filter) cation determination. All aliquots were stored in a refrigerator at 1°C until analysis.

3.2 Aqueous Geochemical Analyses

Major cations and trace metals were analyzed via inductively coupled plasma-optical emission spectrometry (Perkin Elmer Optima 2100 DV) and inductively coupled plasma-mass spectrometry (Elan 6100) utilizing EPA methods 200.7 and 200.8. Ultra-high purity nitric acid was used in sample and calibration preparation prior to sample analysis. Internal standards (Sc, Ge, Bi, and In) were added to samples and standards to correct for matrix effects. Standard Reference Material (SRM) 1643e Trace Elements in Water was used to check the accuracy of the multi-element calibrations. Inorganic anion samples were analyzed by ion chromatography (IC) following EPA method 300 on a Dionex DX-600 system. Aqueous geochemical results are presented in Appendix A.

3.3 SEM characterization

Analytical electron microscopy was performed using a FEI™ Inspect F scanning electron microscope (SEM). All samples were Au/Pd-coated prior to SEM analysis. Imaging with the SEM was performed using a 5.0 kV accelerating voltage and 1.5 spot size. Energy dispersive X-ray spectroscopy (EDX) was performed at 30 kV and a 3.0 spot size.

3.4 Electron Microprobe analyses

Electron microprobe (EMP) analyses were performed at the University of Oklahoma using a Cameca SX50 electron microprobe equipped with five wavelength-dispersive spectrometers and

PGT PRISM 2000 energy-dispersive X-ray detector. Petrographic characterization was performed by backscattered electron imaging coupled with energy-dispersive X-ray analysis, using beam conditions of 20 kV acceleration and 20 nA sample current. Quantitative analysis was performed by wavelength-dispersive spectrometry using 20 kV accelerating voltage, 20 nA beam current, and 2 µm spot size. Matrix corrections employed the PAP algorithm (Pouchou and Pichoir 1985), with oxygen content calculated by stoichiometry. Counting times were 20 seconds on peak for all elements, yielding minimum levels of detection (calculated at 3-σ above mean background) in the range of 0.01 to 0.03 wt. % of the oxides for all components except F (0.16 wt. %). All standards for elements in the silicates were analyzed using 30 second count times on peak, using K-alpha emissions. The standards and oxide detection limits are presented in Appendix B, with analytical data presented in Appendix C.

3.5 XRD Analyses

X-ray diffraction (XRD) analyses of experimental materials determined mineral compositions. Each sample was ground with 20 wt. % corundum (Al_2O_3) for quantitative XRD analysis of the bulk rock (Chung 1974). XRD measurements were conducted with a XPERT-PRO diffractometer using Cu-Kα radiation. Data were collected from 6 to 70 °2θ with a 0.02 º2θ step-size and count times of 8 to 12 seconds per step. Phase identification was accomplished utilizing the program HighScorePlus provided with the Panalytical Expert Pro apparatus at the Bureau of Geology and Mineral Resources on the campus of New Mexico Tech. Standard determinations of background, peak identification, and K*α2* stripping were employed prior to phase identification. Phase identification was aided by selecting known phases previously determined by electron microprobe at another facility. Cold Seal reaction samples were quantified and are displayed in Appendix D

The quantification chart is just a graphical representation of the phase or component weight percentages. The quantification from the RIR values of the accepted reference patterns according to the Chung method (1974) has second priority; the quantification chart shows by default the weight percentages of the actual, measured sample.

The semi-quantitative analysis in HighScore works on basis of the RIR (Reference Intensity Ratio) values (often called I/Ic values). It determines the estimated mass fractions of the identified phases. This method is known as the normalized RIR method and was published by

CHUNG (1974) and others. Sometimes it is less accurately called the adiabatic or matrix flushing model.

The normalization used in this method assumes that the sum of all identified phases is 100%. This means, there are no unidentified crystalline phases nor an amorphous phase present in the sample. Only under these conditions can meaningful semi-quantitative results be obtained. If not all phases are identified, the result is still a good estimate of the relative mass fractions of the identified phases.

Theoretically this method gives exact results. Practically speaking however, several sources of errors prohibit an accurate result. The main errors are:

1.) The RIR values from the reference database:
The RIR values are based on the relative net peak height ratio of the strongest line (Irel= 100%) of the phase and of the strongest line of corundum, measured with copper Kα radiation in a mixture of equal weight percentages. RIR values from the literature (or from the reference database) are known to be inaccurate. The simple stick-pattern approach only works when all peaks have the same FWHM. The peak area is usually a better measure of the diffraction power of a phase. Micro-absorption and texture effects can also jeopardize the determination of the proper intensity ratio.

2.) The scale factor values:
The relative intensity of each phase is given by the scale factor. By definition the measured intensity of the strongest line of each phase should be used to calculate the scale factor. However, in HighScore the scale factor is determined by a least-squares fit through all matching reference pattern lines. This counteracts texture effects to a certain extent, but does not follow the original definition.

4. Results

At present, characterization of the "base of seals experiment (runs DB1 and DB2, 150 C, 300 bar) are limited to aqueous geochemistry only. Complete data analyses for the two month runs are shown in Appendix A, Tables A.1 (CaCl brine) and A.2 (NaCl brine). Graphical displays of the data are also included. **Electron microprobe analyses, quantitative XRD and SEM imaging have not yet been obtained.**

The second experiment (base of hole – canister rupture due to hole collapse, 400 ^{o}C, 1 Kb) have been fully characterized. Electron microprobe analyses of the mineral phases are presented in Appendix C. These include data for the NaCl brine (DBS-1), CaCl brine (DBS-12), and Cs/Ca/NaCl brine (DBS-17). XRD mineral identification and semi quantitative percentages of

minerals present are listed in Appendix D, along with powder diffraction spectra. SEM images and mineral identification of the three brine experiments are presented in Appendix E.

5. Discussion

5.1 Base of Seals Experiment

The intent of the "base of seals" experiment (runs DB1 and DB2, 150 C, 300 bar) was to determine stability of both clay and zeolite phases in the bentonite clay. Although the run products are not yet characterized, we believe that the mineralogy would be similar to the EBS experiments detailed in Caporuscio, et.al. (2015). Since temperatures are lower in the "base of seals" there should be no illitization processes in effect. This is due primarily due to the bulk chemistry of the starting bentonite material and lack of potassium in the brine. In a similar manner, there should be remnant clinoptilolite and incipient analcime formation only.

Aqueous geochemistry data for the base of seals experiment (runs DB1 and DB2, 150 C, 300 bar) as displayed in the Appendix A graphs indicate some interesting trends. We will focus on the cations Ca, Mg, Na, Fe, and SiO_2 as an indicator of silica mineral precipitation / dissolution. The closest match of cation behavior is that of Fe and SiO_2 in both experiments (DB1 [NaCl brine experiment] and DB2 [CaCl brine experiment]). This may suggest that there is an Fe silicate mineral first precipitating and then dissolving in both runs. The other cation trends are not so simple. Both DB1 (NaCl brine experiment) and DB2 (CaCl brine experiment) show precipitation of Ca beginning in the third week. The SiO_2 trends differ for the two experimental "base of seals" runs. DB1 shows an increase in both SiO_2 in solution and in precipitation during the course of the run. In contrast, the SiO_2 values of Experiment DB2 are inversely related. The Mg, Na and K cations in both experiments do not show trends that link to SiO2, nor the anions chloride, bromide, or sulfate.

The "base of seals" experiment (runs DB1 and DB2, 150 C, 300 bar) will be further characterized in FY17 to determine the stability of clays and zeolites with the use of SEM, QXRD, and EMP analyses.

5.2 Bottom of Deep Borehole Experiment

The two main objects of the of CS experiments (400 C, 1 KB) were to investigate 1) if it was possible to create a Cs zeolite in the event of a canister rupture and 2) if a backfill bentonite surrounding the canisters would undergo substantial mineralogical phase changes.

Pollucite ($CsAlSi_2O_6$) is isotypic with anhydrous Analcime ($NaAlSi_2O_6$) and Wairakite ($CaAlSi_2O_6$), in addition to forming a complete solid solution with Analcime. The complete end member of Pollucite is anhydrous (Teertstra and Cerny 1995). At room conditions Pollucite is cubic with Cesium, Na, and H_2O in the extra-framework content. In synthetic Pollucite, $Cs_{16}Al_{16}Si_{32}O_{96}$, was reported at room conditions to have tetragonal symmetry (Xu et al. 2002). H_2O and Cesium share the only extra-framework site in the 6-member ring and Na in the distorted 8-member ring of tetrahedral that connect the 6mR-channels (Beger 1969). The amount of water is only 0-4 wt. % in Pollucite and does not completely dehydrate till 640°C but also showed no weight loss below 300°C (Fleischer and Ksanda 1940). It does not uptake water from the air after dehydration, unlike most zeolites. For uses in nuclear waste, Pollucite is able to retain Cs when immersed in a fluid phase and even under hydrothermal conditions. Synthetic cubic Pollucite preserves its crystallinity at least up to 1197 at room pressure. There is not a phase change reported between 17°C and 1197°C. According to Gatta et al. (2008a) there is a phase change at 5.4 kbar to 7.8 kbar but the transition is reversible and is consistent with the high-*P* polymorph of leucite. The polymorph of Pollucite is more compressible than the low-*P* polymorph but not as compressible as analcime. Past experiments revealed a solid solution of Analcime and Wairakite and thus it was of interest to observe if Cs would incorporate into the zeolite structure. This is a very important observation since Gatta, et. al. (2009) state on the stability of pollucite "the significantly large amount of Cs hosted in this material (Cs2O ~ 30 wt.%), the immobility of Cs at high-temperature and high-pressure conditions (related to the configuration of the Cs-polyhedron and its bonding environment and to the small dimension of the micropores—"free diameters"—where the Cs-sites lie, O ↔ O6mR, Table 2) and the extremely low leaching rate of Cs, make of this open-framework silicate a functional material with potential use for fixation and deposition of Cs radioisotopes". Therefore, our experimental result that a pollucite rich zeolite can be created from precursor bentonite backfill has significant implications for repository design.

The temperatures used for the CS experiments were higher than the base of seals experiments but correlate well and transition into the Hornfels Facies. In our cold seal experiments (DBS17), a Cs zeolite was found with a chemical composition of $(Ca_{0.2}Na_{0.095}Cs_{0.22})Al_{0.8}Si_{2.17}O_6$ and a Si/Al ratio of 2.58 (Table 1). This equates to a solid solution composition of $An_{18.3}Wrk_{39}Pol_{42.7}$ (Figure 8).

Data for Analcime structure zeolite in sample DBS17 (Cs/Ca/NaCl brine)

SiO_2	**56.64**
Al_2O_3	18.63
FeO	0.68
MnO	0.01
MgO	0.05
CaO	4.95
Na_2O	1.27
K_2O	0.05
Cs_2O	13.56
Cl	0.2
F	0.01
O=Hal	-0.05
TOTAL	96.01

Table 1. Average of 30 EMP analyses for analcime structure zeolite produced in experiment DBS17. This equates to a Si/Al ratio of 2.58. Based on cation extrapolation from the EMP data, this zeolite has the following end-member composition - $An_{18.3}Wrk_{39}Pol_{42.7}$

According to the XRD data, there was 5.9% Analcime-Wairakite and 14.9% Pollucite, confirming the presences of a Cs bearing zeolite and one in abundance (Figure 9). Along with the Cs zeolite of sample DBS17, microprobe and QXRD data for sample DBS12 indicate that there is chlorite, plagioclase (anorthite), ferrosilite, amphibole, and clinozoisite. This is an expected mineral assemblage as indicated in Figure 10. The temperatures used for the CS experiments were high but correlate well and transition into the Hornfels / Green Schist facies (Figure 11).

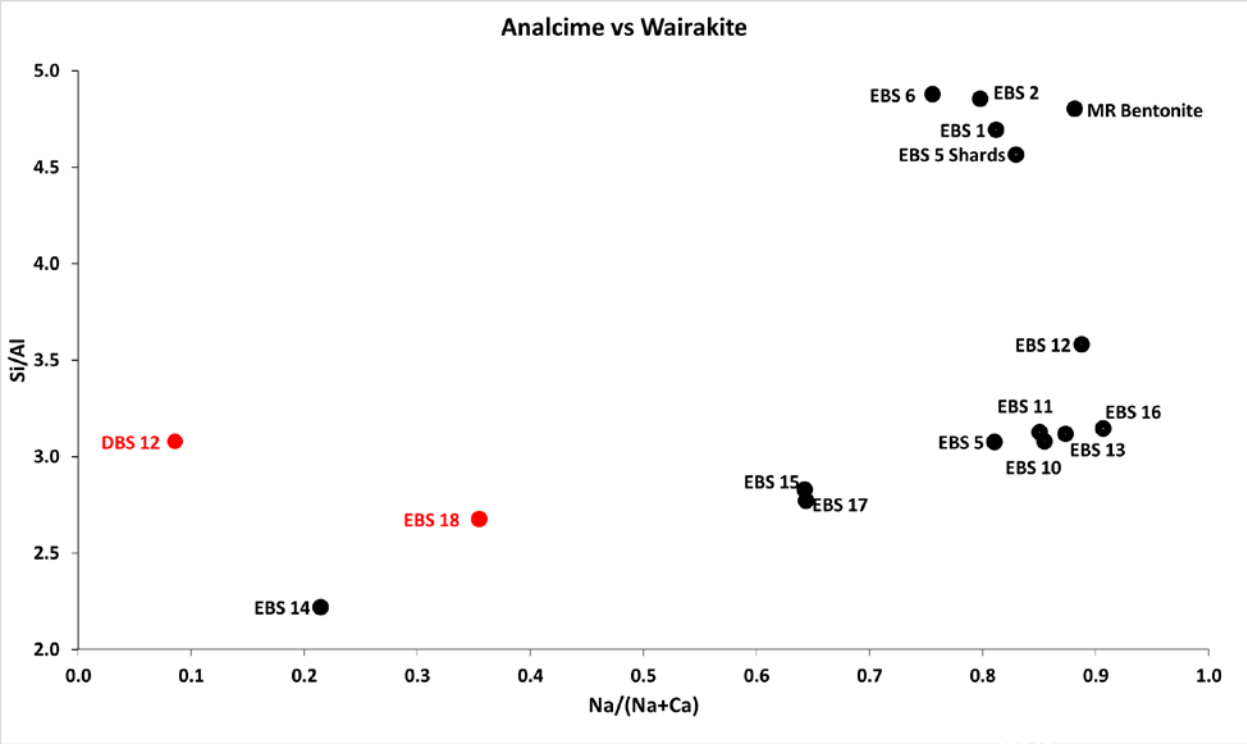

Figure 8: DBS experiments plotted against past EBS experiments

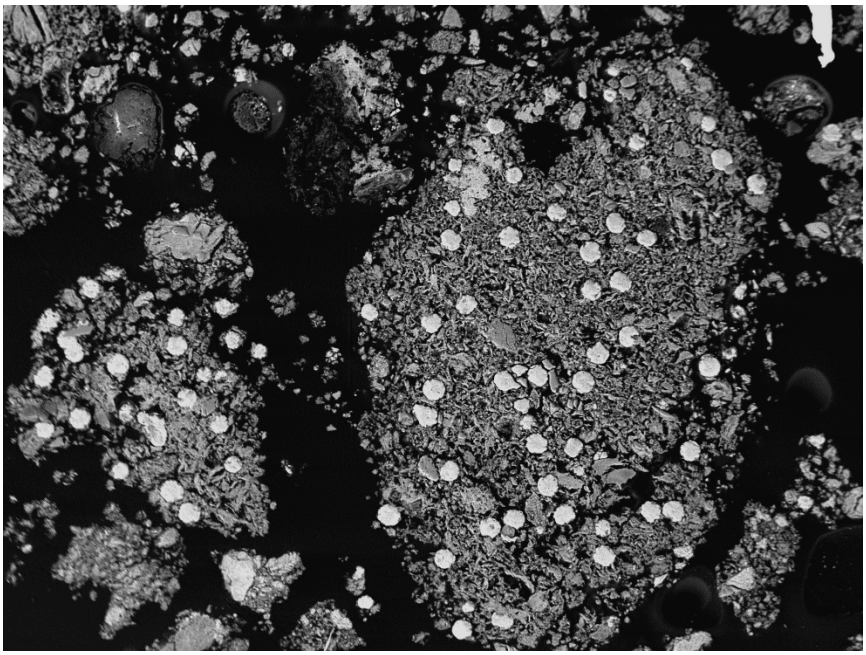

Figure 9. Backscattered image of sample DBS-17. Abundant white circular minerals are Cs-bearing analcime (average diameter 20 micron).

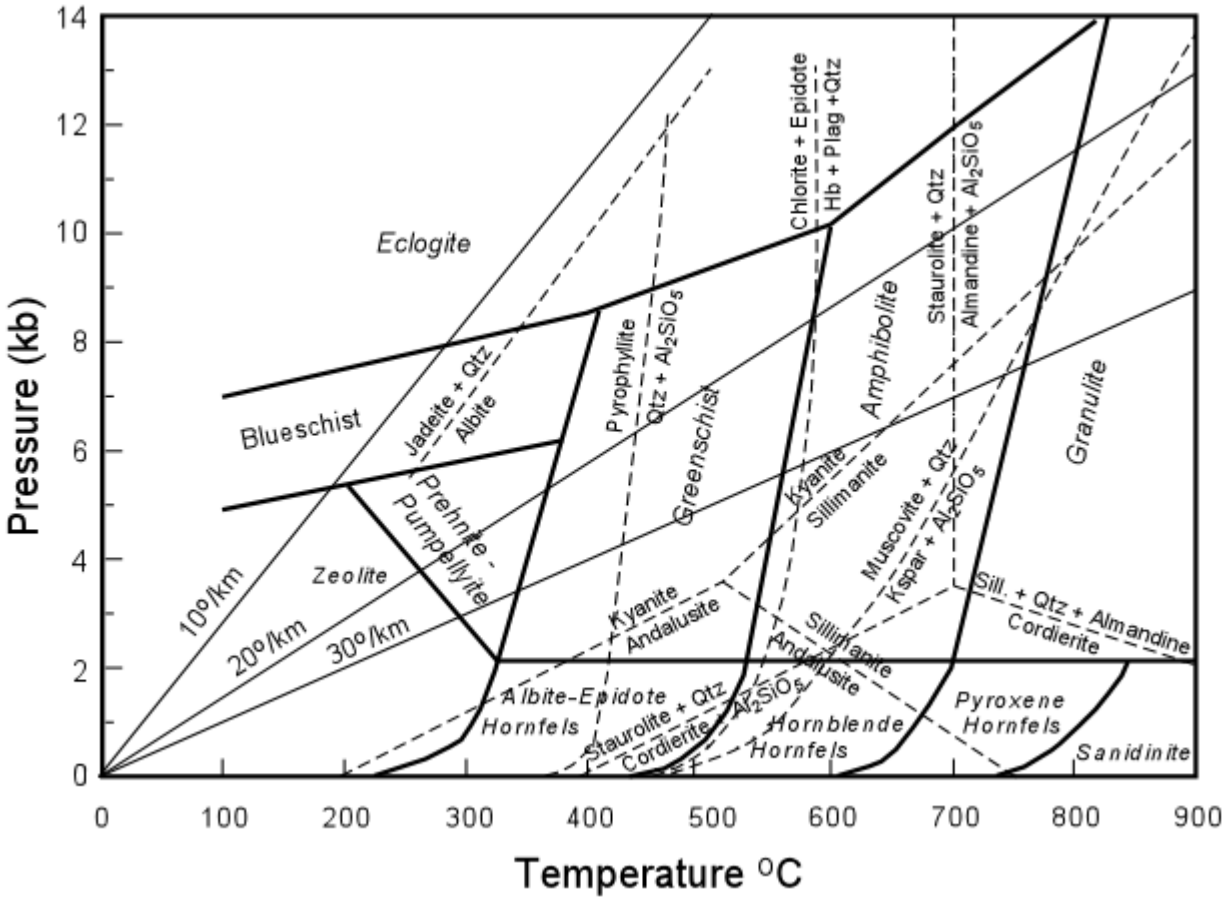

Figure 10. Mineral assemblages expected at various pressure-temperature realms. The "bottom of borehole" experiments would fall into the Albite-Epidote Hornfels metamorphic facies. Probe data for DBS12 agrees with this interpretation. Figure from Tulane.edu: Metamorphic Rocks – Classification, Field Gradients, & Facies

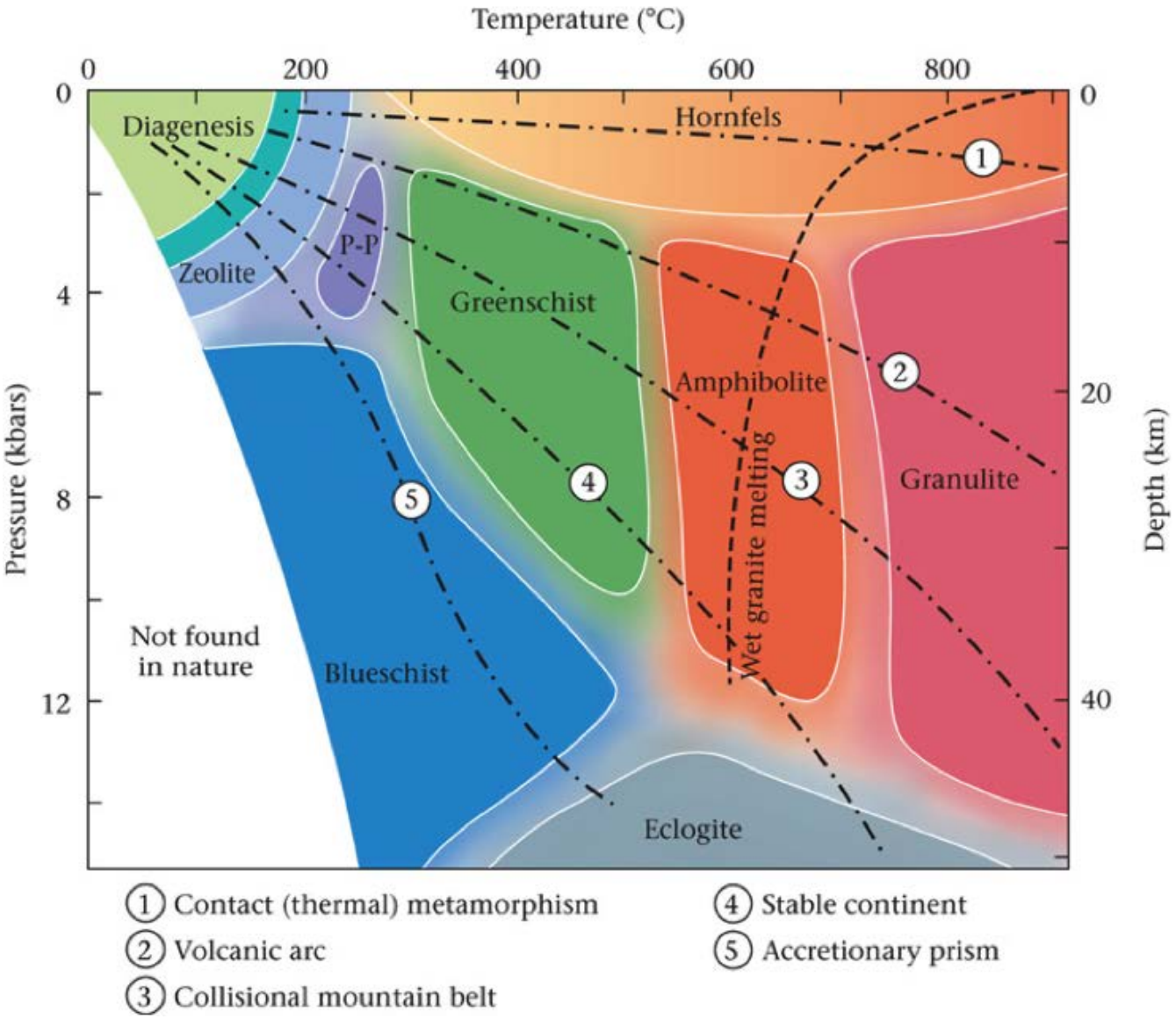

Figure 11. Metamorphic Facies diagram (From:luckysci: Metamorphic rocks, minerals, grade, and facies). Our "base of boreholes" experiments (400 ^{o}C and 1 Kbar) exist in the Hornfels Facies along the contact metamorphism trend.

At present, the high P, T experiment mimicking "bottom of Deep Borehole" with NaCl brine has provided ambiguous results. We believe that the gold capsules ruptured during the experiments and have rerun the samples (DBS20-22). These new samples have not been fully characterized yet. However, they should have a mineralogy assemblage (plagioclase-zeolite-chlorite-amphibole-pyroxene-epidote) in line with the CaCl and Cs/Ca/Na brine experiments (see Appendix C (EMP analyses – DBS12) and Appendix D (DBS12 & DBS18). Select SEM images

are provided in Appendix E. These images document the Hornfels facies assemblage minerals produced in all the "bottom of Deep Borehole" experiments.

To summarize the Deep Borehole experiments for FY16, the "Base of Seals" experiments (150 ^{o}C, 300 bar) have been completed and water chemistry has been analyzed. However further characterization (XRD, EMP, SEM) of the mineral phases will be completed in FY17. The "Bottom of Borehole" experiments have been run and the mineralogical characterization is essentially complete. These experiments have shown that there are significant mineral phase changes at 400 ^{o}C and 1 Kbar pressure. The results are 1) there are wholesale mineral phase changes at elevated P, T, namely bentonite clay (including clinoptilolite and remnant glass) change to feldspar-quartz-pyroxene-amphibole-epidote/clinozoisite-chlorite-analcime type zeolite) and 2) that Cs is readily incorporated into the analcime structure if a canister ruptures early during the emplacement phase and bentonite backfill is emplaced.

6. Conclusions and further work

Proof of concept experiments for deep borehole disposal of CsCl waste forms have revealed multiple intriguing mineralogic changes. Even though the base of seals experiments are not analytically characterized at this point in time, the run products extracted were still dominated by clay mineralogy. The bottom of borehole experiments indicate a significant shift in mineralogy from clay and zeolite based minerals (Diagenetic) to a Hornfels facies mineralogy (feldspar, epidote, pyroxene, amphibole, chlorite, analcime). Such mineral phase changes will have an impact on chemistry, mechanical properties, and radionuclide sorption. The high temperature, pressure experiment (400 ^{o}C, 1 Kbar) designed to mimic a canister failure at the bottom of a borehole resulted in the growth of a Cs-rich analcime from a precursor bentonite backfill. This analcime contained 13.6 wt. % Cs_2O. This is the first time that Cs-analcime has been produced from a bentonite material buffer in an experimental setting. Although further work is needed to determine the stability range of this mineral, it may be possible to consider using bentonite backfill around the canisters as a radionuclide getter.

Currently we are preparing samples for micro probe, XRD and SEM to characterize samples DB1, DB2 (base of seals experiments), and DBS NaCl mineralogy. With further Deep Boreholes funding the experiments just mentioned will be analyzed. Increased funding will allow for experiments to further delimit Cs-rich analcime phase stability over a pressure temperature range

7. References

Anderson, V.K., 2004, *An Evaluation of the Feasibility of Disposal of Nuclear Waste in Very Deep Boreholes*. Dept. of Nuclear Engineering. Cambridge, MA, MIT.

Amec, 2014 Sealing deep site investigation boreholes: Phase 1 report. AMEC, Oxford, Great Briton, RWMD/03/042, pp 200

Arnold, B.W., P.V. Brady, S.J. Bauer, C. Herrick, S. Pye, and J. Finger, 2011, *Reference Design and Operations for Deep Borehole Disposal of High-Level Radioactive Waste.* SAND2011-6749. Albuquerque, NM: Sandia National Laboratories.

Arnold, B.W., P.V. Brady, Altman, S., Vaughn, P., Nielson, D., lee, J., Gibb, F., Mariner, P., Travis, K., Halsey, W., Beswick, J., and Tillman, J. 2013 Deep Borehole Disposal Research: Demonstration Site Selection Guidelines, Borehole Seals Design, and R&D Needs. SAND2013-9490P. Albuquerque, NM: Sandia National Laboratories.

Arnold, B. W., and T. Hadgu, 2013, Thermal-hydrologic modeling of a deep borehole disposal system, *Proceedings of the 14th International High-Level Radioactive Waste Management Conference, April 28-May 2, 2013,* Albuquerque, NM.

Arnold, B.W., Brady, P., Gibb, F.G.F., N.A. McTaggart, K.P. Travis, and D. Burley, 2008, A model for heat flow in deep borehole disposals of high-level nuclear wastes. *Journal of Geophysical Research,* **113,** http://dx.doi.org/10.1029/2007JB005081

Brady, P.V., B.W. Arnold, G.A. Freeze, P.N. Swift, S.J. Bauer, J.L. Kanney, R.P. Rechard, J.S. Stein, 2009, *Deep Borehole Disposal of High-Level Radioactive Waste*, SAND2009-4401, Albuquerque, NM, Sandia National Laboratories.

Beger, R.M. (1969) The crystal structure and chemical composition of pollucite. Zeitschrift für Kristallographie, 129, 280–302.

Caporuscio, F.A., Cheshire, M.C., Palaich, S., Norskog, K., and Jove Colon, C. 2015, Summary of baseline experiments for generic repository engineered barriers. LA-UR 15-26110, Los Alamos National Laboratory, Los Alamos, NM

Cheshire, M.C., Caporuscio, F.A., Jove-Colon, C., and McCarney, M.K. (2014) Bentonite Clay Evolution at Elevated Pressures and Temperatures: An experimental study for generic nuclear repositories. American Mineralogist, V99, pp1662-1675

Fleischer, M. and Ksanda, C.J. (1940) Dehydration of pollucite. American Mineralogist, 25, 666–672.

Gatta, G.D., Rotiroti, N., Boffa Ballaran, T., and Pavese, A. (2008a) Leucite at high-pressure: Elastic behavior, phase stability and petrological implications. American Mineralogist, 93, 1588–1596.

Gatta, G.D., Rotiroti, N., Ballaran, T.B., Sanchez-Valle, C., and Pavese, A. (2009) Elastic behavior and phase stability of pollucite, a potential host for nuclear waste. American Mineralogist, V94, pp1137-1143

Chung, F.H., 1974. Quantitative interpretation of X-ray diffraction patterns, I. Matrix-flushing method of quantitative multicomponent analysis, J. Appl. Cryst., 7, 513 – 519

Gibb, F.G.F., N.A. McTaggart, K.P. Travis, and D. Burley, 2008a, A model for heat flow in deep borehole disposals of high-level nuclear wastes. *Journal of Geophysical Research,* **113,** http://dx.doi.org/10.1029/2007JB005081

Heiken, G., G. Woldegabriel, R. Morley, H. Plannerer, J. Rowley, 1996, *Disposition of Excess Weapon Plutonium in Deep Boreholes – Site Selection Handbook*. Los Alamos, NM, Los Alamos National Laboratory.

Juhlin, C. and H. Sandstedt, 1989, *Storage of Nuclear Waste in Very Deep Boreholes: Feasibility study and assessment of economic potential.* SKB Technical Report, 89-39, Stockholm, Sweden.

Kazumichi Yanagisawa , Mamoru Nishioka & Nakamichi Yamasaki (1987) Immobilization of Cesium into Pollucite Structure by Hydrothermal Hot-Pressing, Journal of Nuclear Science and Technology, 24:1, 51-60, DOI: 10.1080/18811248.1987.9735774

Lucky Sci: Metamorphic rocks, minerals, grade, and facies August 8 2014 [Accessed 2016, July]. http://www.luckysci.com/2014/08/metamorphic-rocks-minerals-grade-and-facies/

Metamorphic Rocks – Classification, Field Graients, &Facies. March 31, 2004, Tulane University: Professor Stephen A. Nelson [accessed 2016 July]

Nirex, 2004, *A Review of the Deep Borehole Disposal Concept*, Report N/108, United Kingdom Nirex Limited

O'Brien, M.T, L.H. Cohen, T.N. Narasimhan, T.L. Simkin, H.A. Wollenberg, W.F. Brace, S. Green, H.P. Platt, 1979, *The Very Deep Hole Concept: Evaluation of an Alternative for Nuclear Waste Disposal*, Berkeley, CA, Lawrence Berkeley Laboratory, LBL-7089

Pouchou, J.L. and Pichoir, F. (1985) "PAP" [illegible] procedure for improved quantitative microanalysis. Microbeam Analysis. Ed. Armstrong, J.T. San Francisco Press, pp. 104-106.

Seyfried, J.R., Janecky, D.R., and Berndt, M.E. (1987) Rocking autoclaves for hydrothermal experiments II. The flexible reaction-cell system. Hydrothermal Experimental Techniques. Eds. Ulmer, G.C. and Barnes, H.L. John Wiley & Sons, pp. 216 – 239.

Teertstra, D.K. and Černý, P. (1995) First natural occurrences of end-member pollucite: A product of low-temperature reequilibration. European Journal of Mineralogy, 7, 1137–1148.

Woodward – Clyde Consultants, 1983, *Very Deep Hole Systems Engineering Studies.* Columbus, OH, ONWI.

Xu, H., Navrotsky, A., Balmer, M.L., and Su, Y. (2002) Crystal chemistry and phase transitions in substituted pollucites along the CsAlSi2O6-CsTiSi2O6.5 join: A powder synchrotron X-ray diffractometry study. Journal of the American Ceramic Society, 85, 1235–1242.

Appendix A
Water Chemistry

DBL-2 2 Molal CaCl Brine and Bentonite

ID	Date	B	Ba	Ca	Cr	Fe	K	Li
DBL-2 UF	05/04/16	5.567892	20.16686	63740.1896	<0.02	87.22797	184.9998	0.692425
DBL-2 F	05/04/16	5.926185	31.56966	68459.50935	<0.02	121.2992	207.0363	0.751671
DBL-2 UF	05/19/16	5.480074	36.34123	60048.75847	<0.02	107.1977	190.4878	0.710078
DBL-2 F	05/19/16	6.440203	21.94959	68501.46425	0.045158	102.4553	217.2813	0.862722
DBL-2 UF	06/02/16	6.304116	28.17157	68627.17282	<0.02	112.9614	212.6246	0.820585
DBL-2 F	06/02/16	5.955124	25.01804	65119.00428	<0.02	123.6963	206.6065	0.766921
DBL-2 UF	06/14/16	6.516296	36.8371	67335.90317	0.0212236	133.2224	221.6684	0.84035
DBL-2 F	06/14/16	6.720482	32.56451	68276.26352	0.0345354	130.3354	222.1794	0.824957
DBL-2 UF	06/15/16	6.393511	32.08393	68475.24505	0.0230542	121.9701	196.9309	0.853399
DBL-2 F	06/15/16	6.39862	32.08995	68854.389	<0.02	123.1435	200.6016	0.858781

ID	Date	Mg	Mn	Na	Si	SiO2	Sr	Zn
DBL-2 UF	05/04/16	100.8531	8.937895	1890.99596	102.85604	220.1119	52.44759	1.972638
DBL-2 F	05/04/16	110.5505	9.746002	2077.169164	155.16776	332.059	56.69451	0.845894
DBL-2 UF	05/19/16	93.32703	9.970832	1834.368571	109.07389	233.4181	50.38735	1.325727
DBL-2 F	05/19/16	107.531	11.22617	2124.508849	68.203964	145.9565	57.04846	1.434492
DBL-2 UF	06/02/16	103.1844	11.76144	2111.158752	73.737768	157.7988	56.0821	1.382316
DBL-2 F	06/02/16	100.3272	11.16444	1979.498727	106.09559	227.0446	53.48343	1.023662
DBL-2 UF	06/14/16	103.6052	12.27281	2063.866762	80.570476	172.4208	56.12805	1.477717
DBL-2 F	06/14/16	103.899	12.17009	2095.427344	98.598792	211.0014	56.38218	1.245918
DBL-2 UF	06/15/16	102.4619	12.18247	2070.551207	40.958098	87.65033	56.52943	0.092481
DBL-2 F	06/15/16	103.5401	12.22604	2057.378412	46.067137	98.58367	56.75731	<0.02

Anions	Date	Bromide	Chloride	Fluoride	Nitrate	Sulfate
DBL-2	05/04/16	9.69	111358.15	<0.5	1.5444	69.28
DBL-2	05/19/16	10.70	120042.32	5.33	2.2130	82.47
DBL-2	06/02/16	11.54	127722.37	<0.5	<0.5	114.40
DBL-2	06/14/16	11.02	122953.86	<0.5	0.2440	100.75
DBL-2	06/15/16	10.61	118863.54	<0.5	0.3571	86.85

DBL-1 2 Molal NaCl Brine and Bentonite								
ID	**Date**	**B**	**Ba**	**Ca**	**Cr**	**Fe**	**K**	**Li**
DBL-1 UF	05/04/16	4.521596	5.782894	353.6657	<0.02	40.46707	146.4957	0.592828
DBL-1 F	05/04/16	4.675159	10.72824	369.4634	<0.02	46.80638	170.0246	0.614333
DBL-1 UF	05/19/16	5.249093	12.94929	382.6718	<0.02	67.64721	153.4305	0.65316
DBL-1 F	05/19/16	5.191848	12.97752	368.7971	0.035135	54.9671	146.6104	0.650996
DBL-1 UF	06/02/16	6.542001	6.84567	421.8395	<0.02	82.33063	180.4145	0.778107
DBL-1 F	06/02/16	5.455468	12.46246	378.8615	<0.02	74.1623	179.5424	0.665822
DBL-1 UF	06/14/16	5.518439	9.643999	369.4812	<0.02	72.15205	149.2496	0.651429
DBL-1 F	06/14/16	5.605277	14.11441	376.2136	0.03659	75.90767	172.9754	0.661087
DBL-1 UF	06/15/16	5.394504	13.7849	369.5299	<0.02	77.34013	150.2391	0.667454
DBL-1 F	06/15/16	4.983216	13.16983	361.5133	<0.02	73.35227	154.7912	0.636852

ID	**Date**	**Mg**	**Mn**	**Na**	**Si**	**SiO2**	**Sr**	**Zn**
DBL-1 UF	05/04/16	81.8253	5.520606	32762.94	76.38821	163.4708	16.43425	5.824501
DBL-1 F	05/04/16	88.53262	5.839451	34256.73	78.85948	168.7593	17.84843	4.928661
DBL-1 UF	05/19/16	87.71477	6.95196	35290.96	119.0985	254.8708	18.36839	2.030216
DBL-1 F	05/19/16	83.90509	6.695404	35281.28	94.34407	201.8963	17.52605	3.246752
DBL-1 UF	06/02/16	97.65716	8.28914	38652.69	141.814	303.4819	19.93642	0.750875
DBL-1 F	06/02/16	85.775	7.376332	34955.65	121.29	259.5605	18.36483	0.487076
DBL-1 UF	06/14/16	82.50916	7.652178	33663.18	121.5827	260.187	17.52242	0.926418
DBL-1 F	06/14/16	84.72138	7.772624	34622.7	126.8629	271.4867	18.13596	1.022985
DBL-1 UF	06/15/16	82.60324	7.510755	34039.15	117.2964	251.0143	17.91152	<0.02
DBL-1 F	06/15/16	81.27215	7.311948	32159.13	106.4058	227.7083	17.31479	<0.02

Anions	**Date**	**Bromide**	**Chloride**	**Nitrate**	**Sulfate**
DBL-1	05/04/16	2.96	58165.73	<0.5	93.89
DBL-1	05/19/16	3.31	62812.12	1.5703	99.32
DBL-1	06/02/16	3.07	60267.12	1.0942	97.96
DBL-1	06/14/16	3.31	58284.30	0.3825	94.43
DBL-1	06/15/16	3.00	62099.59	0.4724	104.56

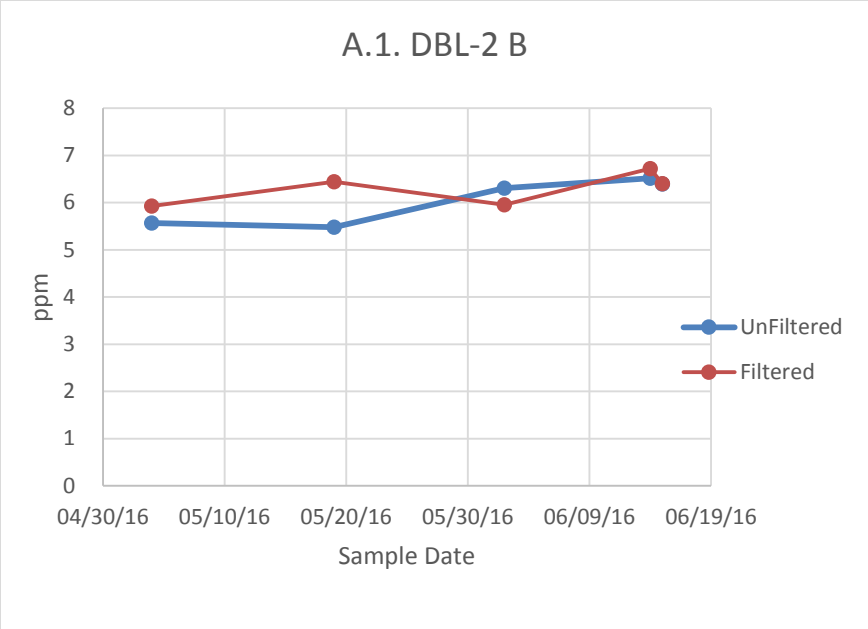
A.1. DBL-2 B
ppm
8
7
6
5
4
3
2
1
0
04/30/16
05/10/16
05/20/16
05/30/16
06/09/16
06/19/16
Sample Date
UnFiltered
Filtered

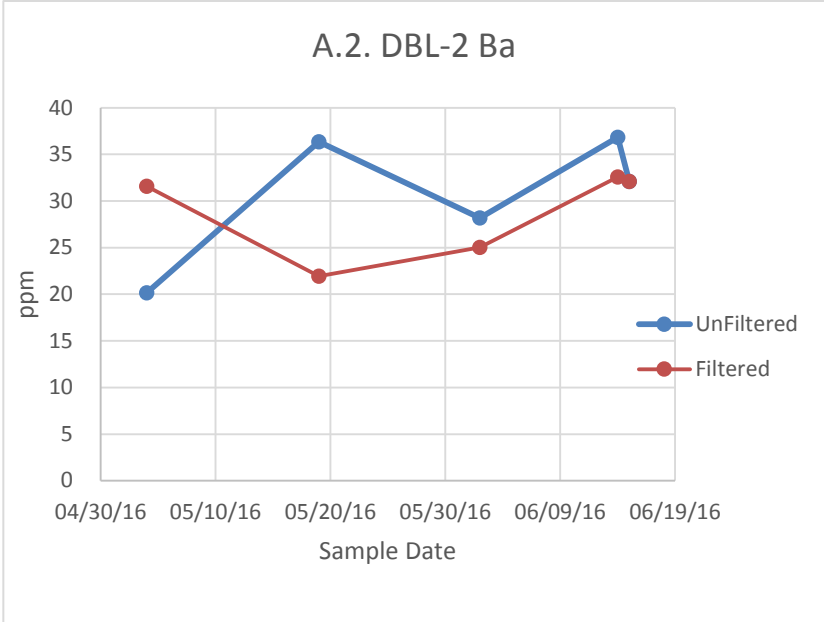
A.2. DBL-2 Ba
ppm
40
35
30
25
20
15
10
5
0
04/30/16
05/10/16
05/20/16
05/30/16
06/09/16
06/19/16
Sample Date
UnFiltered
Filtered

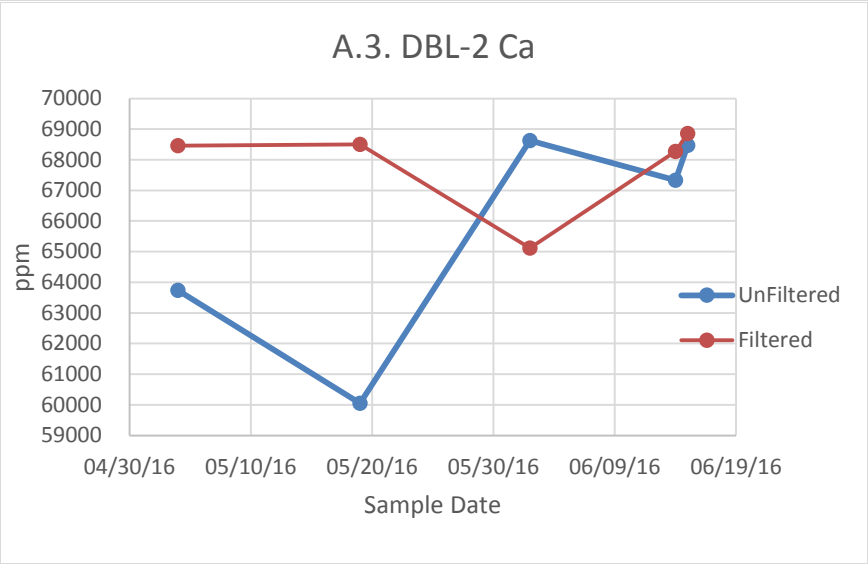
A.3. DBL-2 Ca
ppm
70000
69000
68000
67000
66000
65000
64000
63000
62000
61000
60000
59000
04/30/16
05/10/16
05/20/16
05/30/16
06/09/16
06/19/16
Sample Date
UnFiltered
Filtered

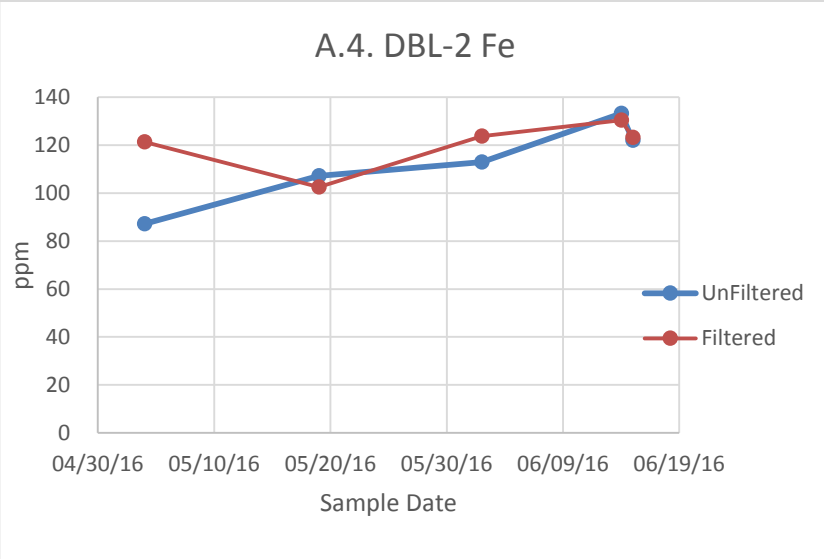
A.4. DBL-2 Fe
ppm
140
120
100
80
60
40
20
0
04/30/16
05/10/16
05/20/16
05/30/16
06/09/16
06/19/16
Sample Date
UnFiltered
Filtered

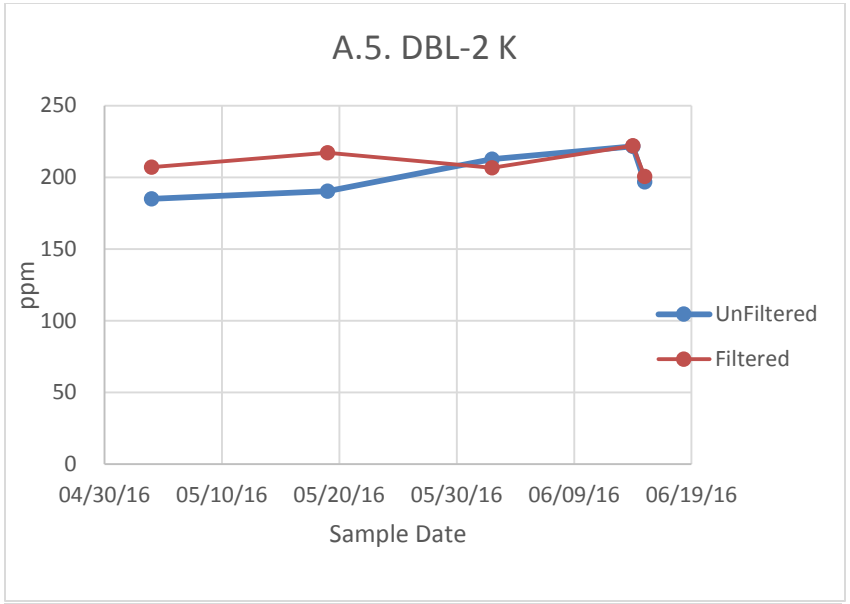
A.5. DBL-2 K
250
200
150
100
50
0
ppm
04/30/16
05/10/16
05/20/16
05/30/16
06/09/16
06/19/16
Sample Date
UnFiltered
Filtered

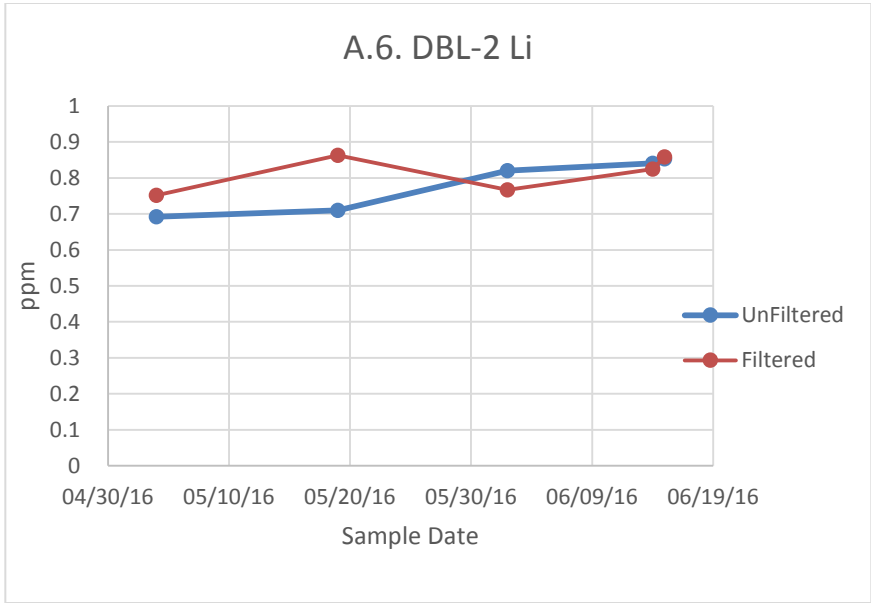
A.6. DBL-2 Li
1
0.9
0.8
0.7
0.6
0.5
0.4
0.3
0.2
0.1
0
ppm
04/30/16
05/10/16
05/20/16
05/30/16
06/09/16
06/19/16
Sample Date
UnFiltered
Filtered

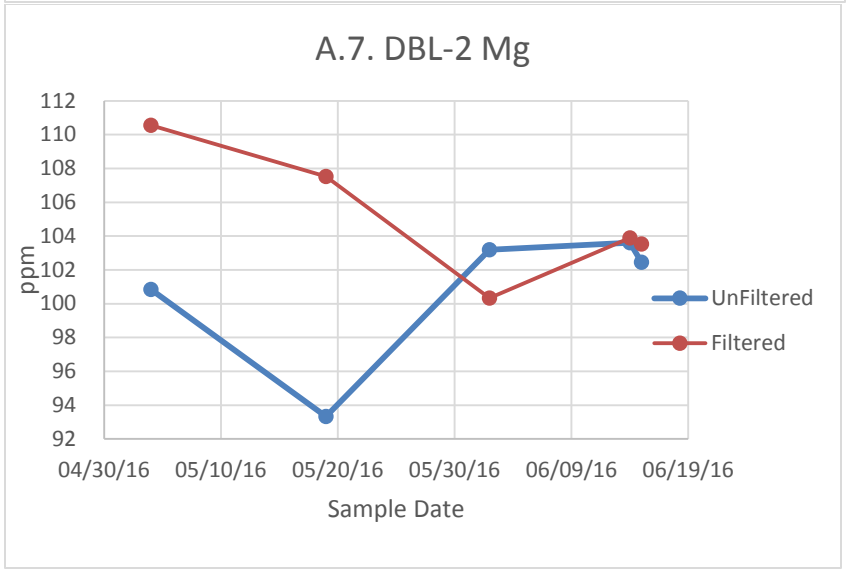
A.7. DBL-2 Mg
112
110
108
106
104
102
100
98
96
94
92
ppm
04/30/16
05/10/16
05/20/16
05/30/16
06/09/16
06/19/16
Sample Date
UnFiltered
Filtered

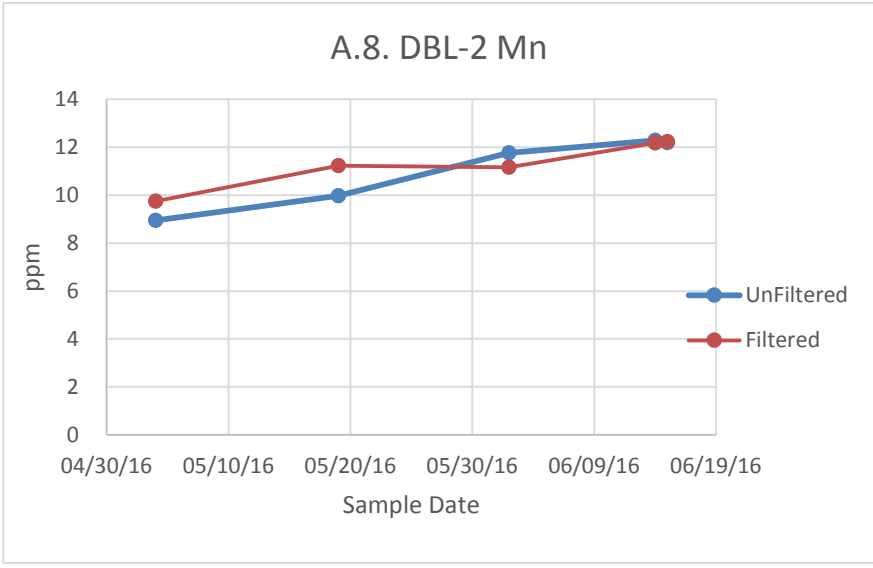
A.8. DBL-2 Mn
14
12
10
8
6
4
2
0
ppm
04/30/16
05/10/16
05/20/16
05/30/16
06/09/16
06/19/16
Sample Date
UnFiltered
Filtered

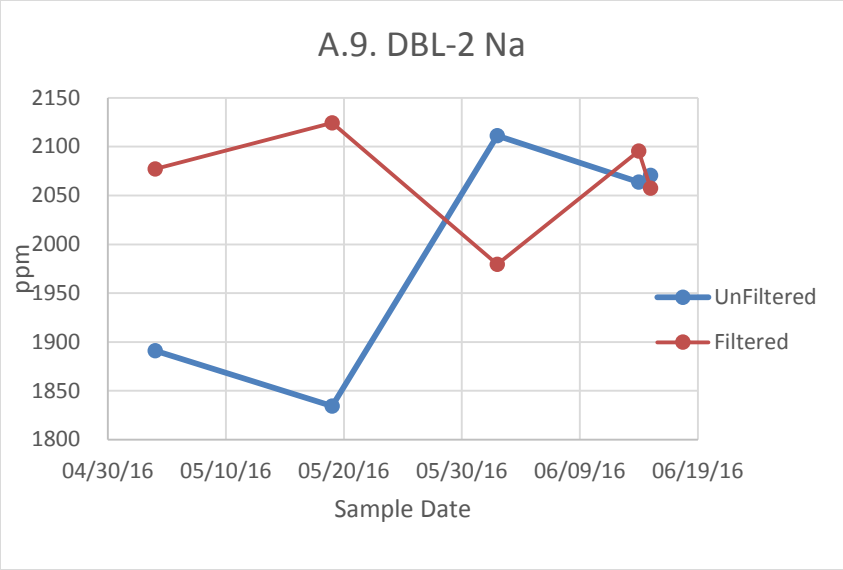
A.9. DBL-2 Na
2150
2100
2050
2000
1950
1900
1850
1800
ppm
04/30/16
05/10/16
05/20/16
05/30/16
06/09/16
06/19/16
Sample Date
UnFiltered
Filtered

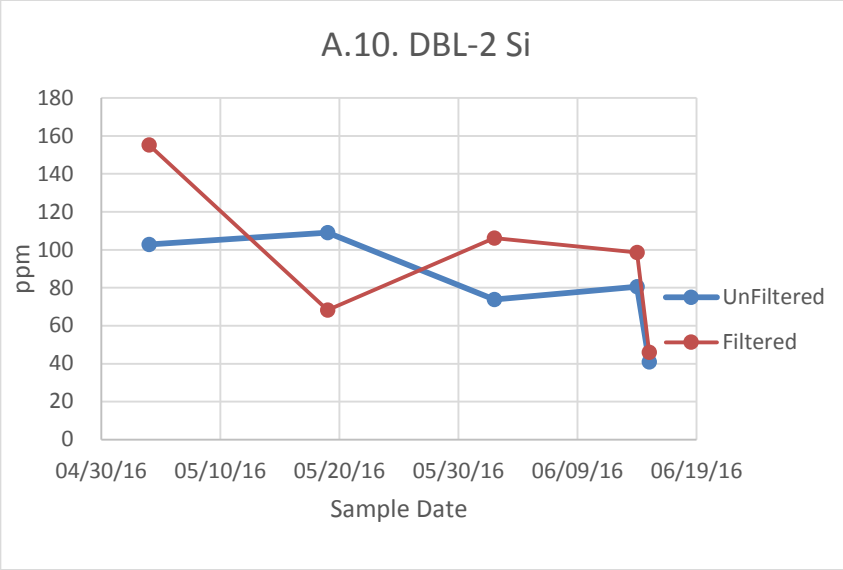
A.10. DBL-2 Si
180
160
140
120
100
80
60
40
20
0
ppm
04/30/16
05/10/16
05/20/16
05/30/16
06/09/16
06/19/16
Sample Date
UnFiltered
Filtered

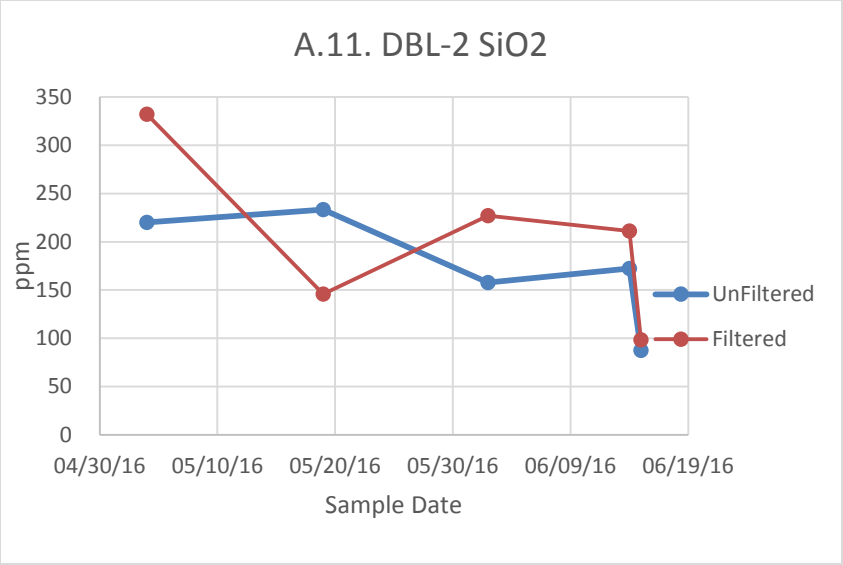
A.11. DBL-2 SiO2
350
300
250
200
150
100
50
0
ppm
04/30/16
05/10/16
05/20/16
05/30/16
06/09/16
06/19/16
Sample Date
UnFiltered
Filtered

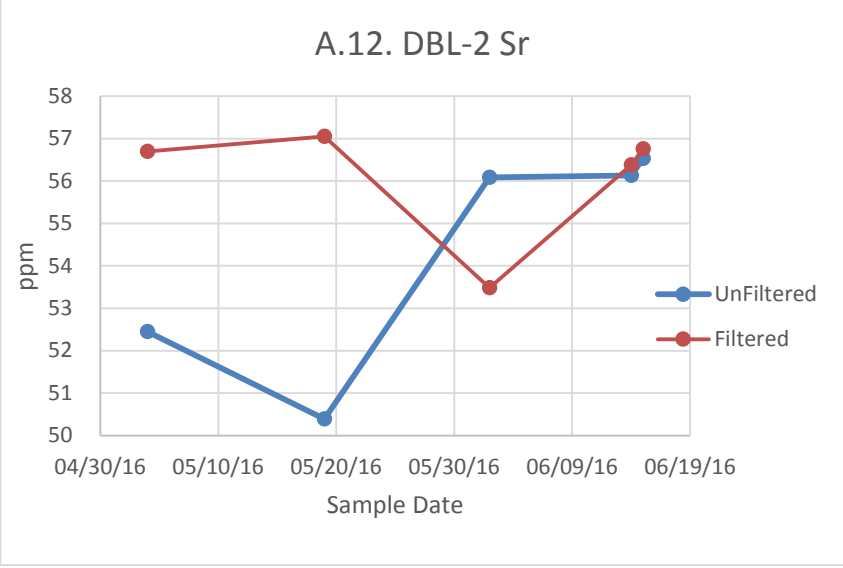
A.12. DBL-2 Sr
58
57
56
55
54
53
52
51
50
ppm
04/30/16
05/10/16
05/20/16
05/30/16
06/09/16
06/19/16
Sample Date
UnFiltered
Filtered

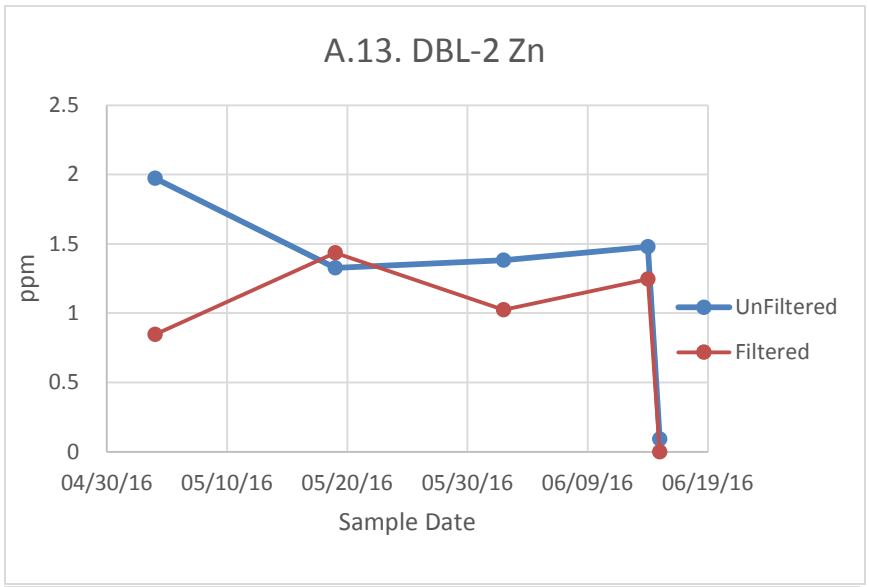
A.13. DBL-2 Zn
2.5
2
1.5
1
0.5
0
ppm
04/30/16
05/10/16
05/20/16
05/30/16
06/09/16
06/19/16
Sample Date
UnFiltered
Filtered

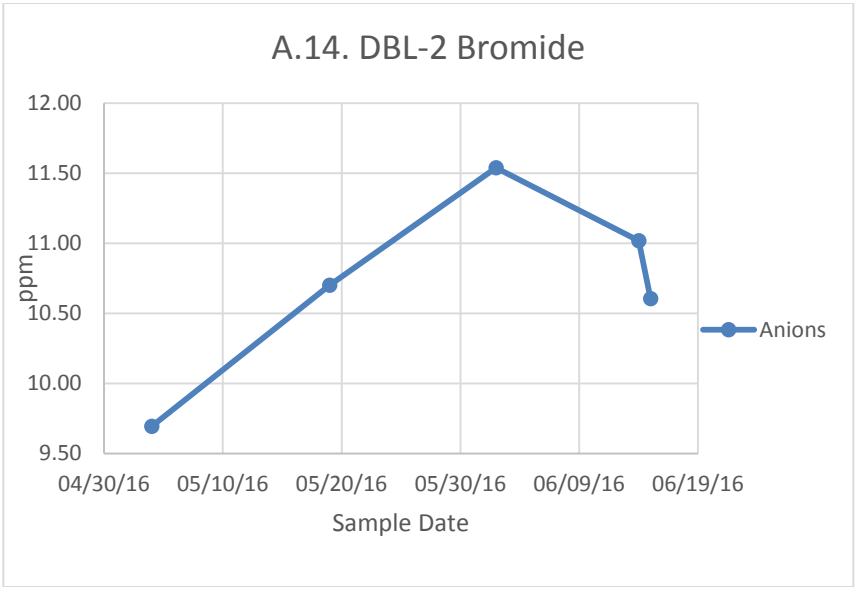
A.14. DBL-2 Bromide
12.00
11.50
11.00
10.50
10.00
9.50
ppm
04/30/16
05/10/16
05/20/16
05/30/16
06/09/16
06/19/16
Sample Date
Anions

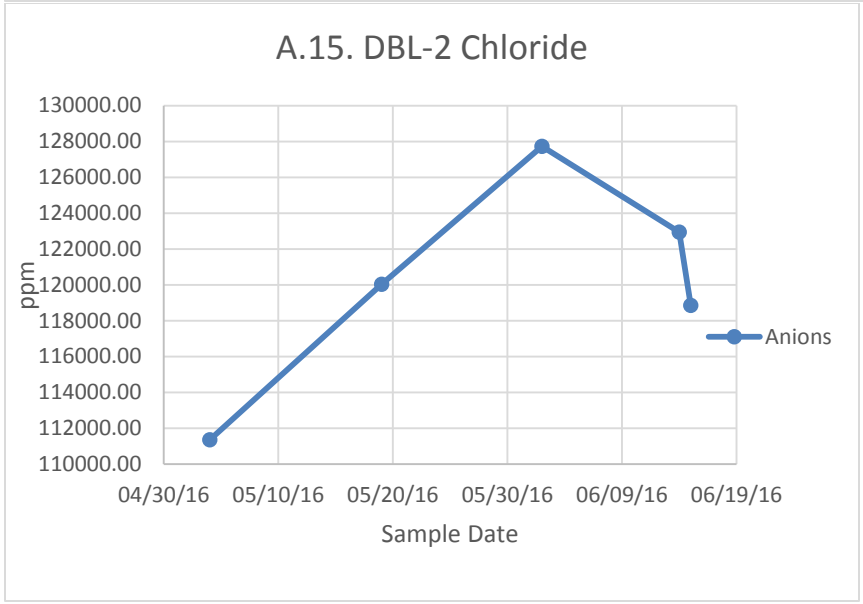
A.15. DBL-2 Chloride
130000.00
128000.00
126000.00
124000.00
122000.00
120000.00
118000.00
116000.00
114000.00
112000.00
110000.00
ppm
04/30/16
05/10/16
05/20/16
05/30/16
06/09/16
06/19/16
Sample Date
Anions

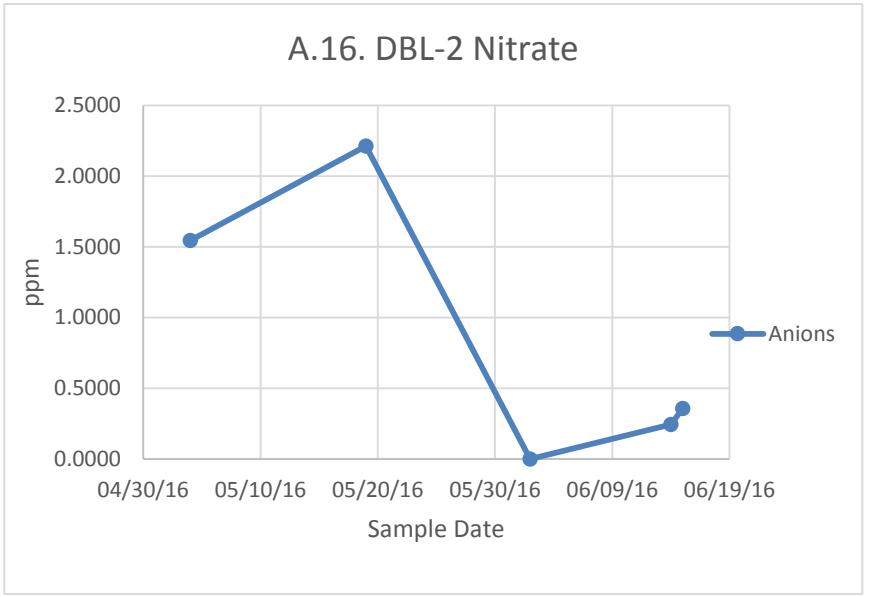
A.16. DBL-2 Nitrate
2.5000
2.0000
1.5000
1.0000
0.5000
0.0000
ppm
04/30/16
05/10/16
05/20/16
05/30/16
06/09/16
06/19/16
Sample Date
Anions

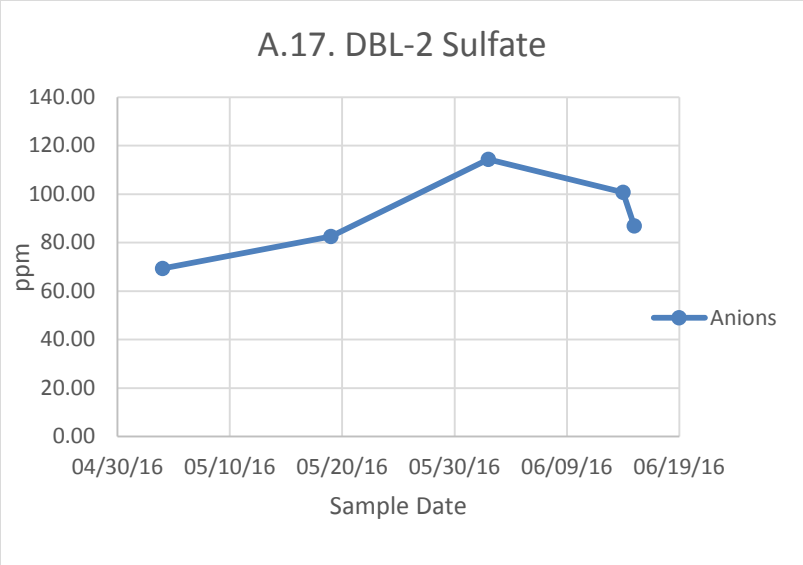
A.17. DBL-2 Sulfate
140.00
120.00
100.00
80.00
60.00
40.00
20.00
0.00
ppm
04/30/16
05/10/16
05/20/16
05/30/16
06/09/16
06/19/16
Sample Date
Anions

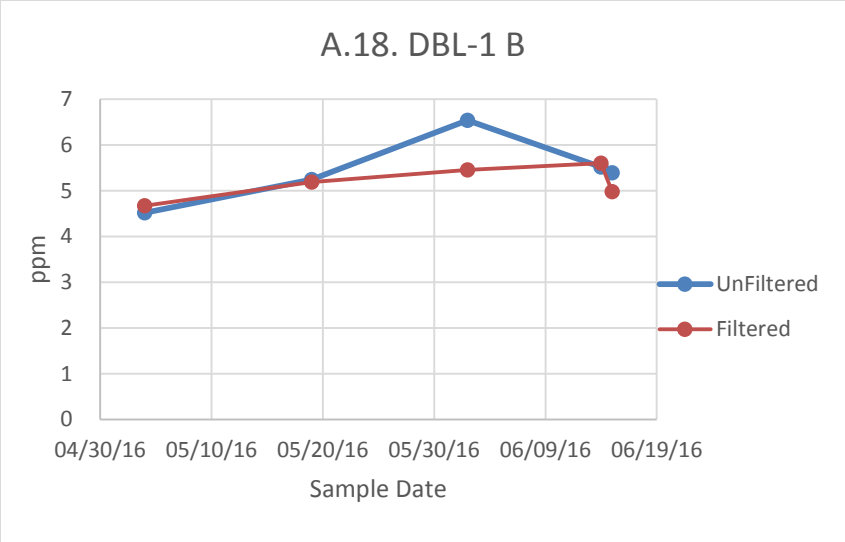
A.18. DBL-1 B
7
6
5
4
3
2
1
0
ppm
04/30/16
05/10/16
05/20/16
05/30/16
06/09/16
06/19/16
Sample Date
UnFiltered
Filtered

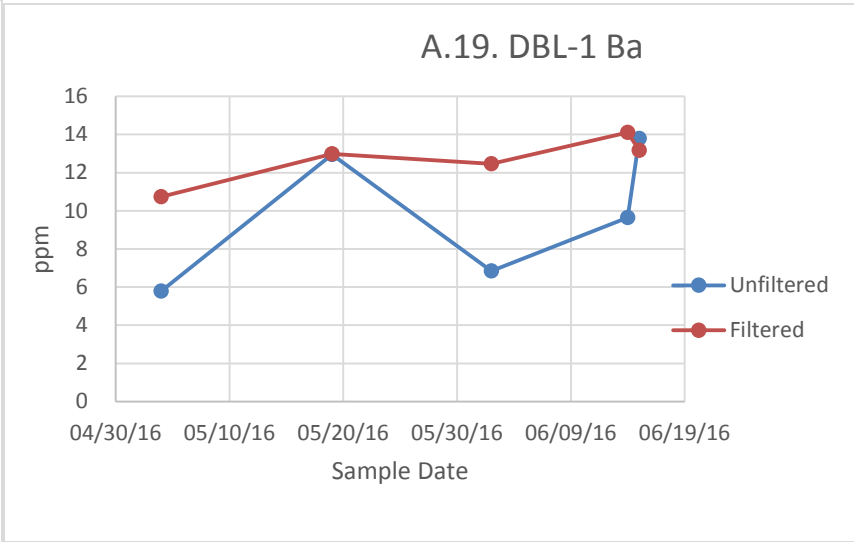
A.19. DBL-1 Ba
16
14
12
10
8
6
4
2
0
ppm
04/30/16
05/10/16
05/20/16
05/30/16
06/09/16
06/19/16
Sample Date
Unfiltered
Filtered

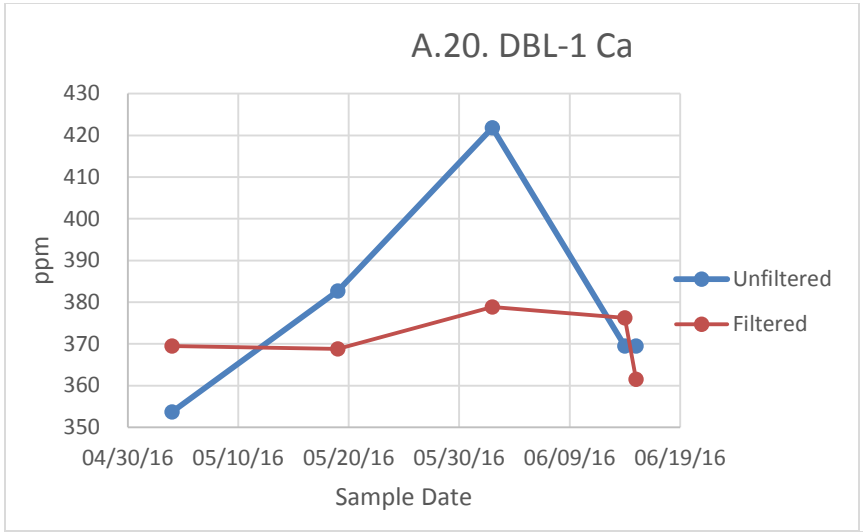
A.20. DBL-1 Ca
ppm
430
420
410
400
390
380
370
360
350
04/30/16
05/10/16
05/20/16
05/30/16
06/09/16
06/19/16
Sample Date
Unfiltered
Filtered

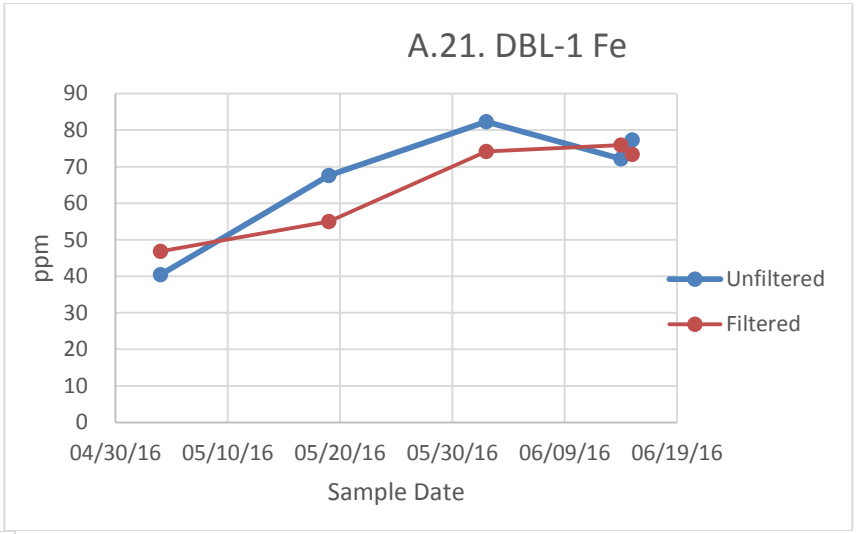
A.21. DBL-1 Fe
ppm
90
80
70
60
50
40
30
20
10
0
04/30/16
05/10/16
05/20/16
05/30/16
06/09/16
06/19/16
Sample Date
Unfiltered
Filtered

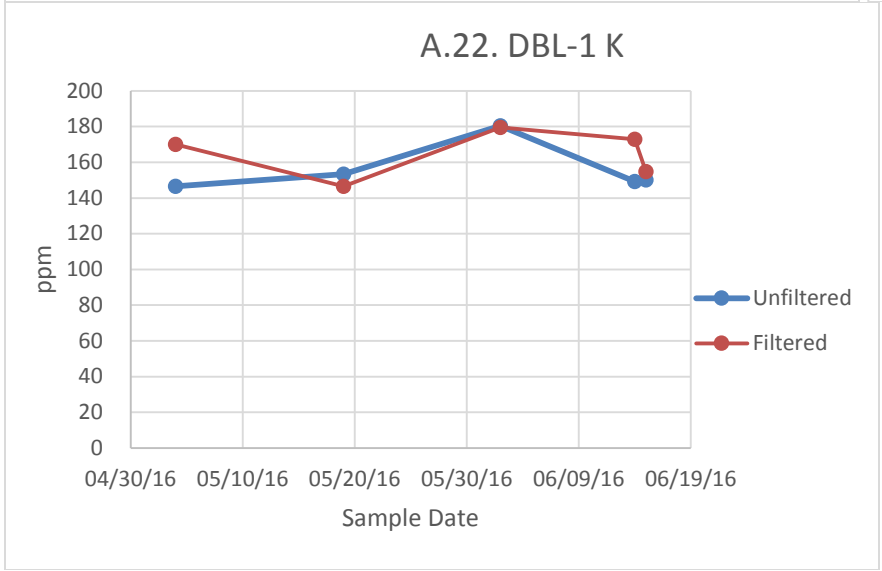
A.22. DBL-1 K
ppm
200
180
160
140
120
100
80
60
40
20
0
04/30/16
05/10/16
05/20/16
05/30/16
06/09/16
06/19/16
Sample Date
Unfiltered
Filtered

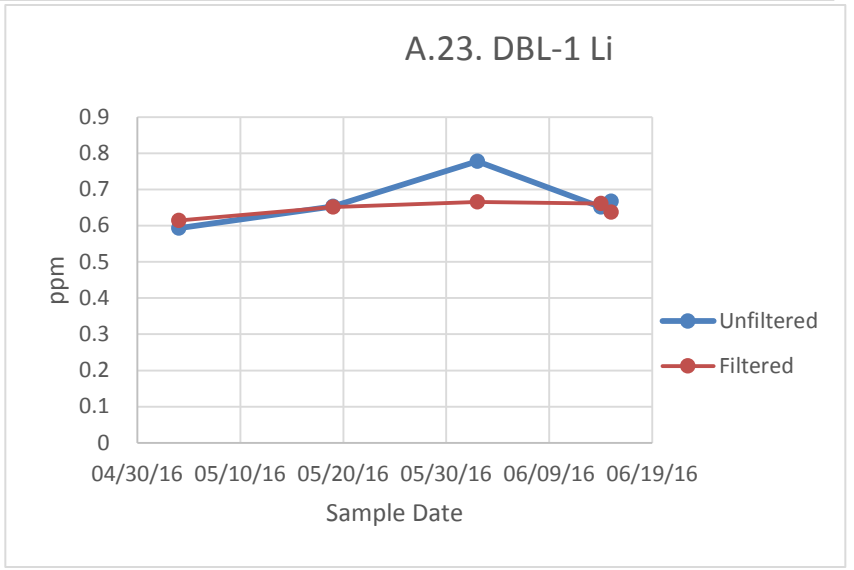
A.23. DBL-1 Li
ppm
0.9
0.8
0.7
0.6
0.5
0.4
0.3
0.2
0.1
0
04/30/16
05/10/16
05/20/16
05/30/16
06/09/16
06/19/16
Sample Date
Unfiltered
Filtered

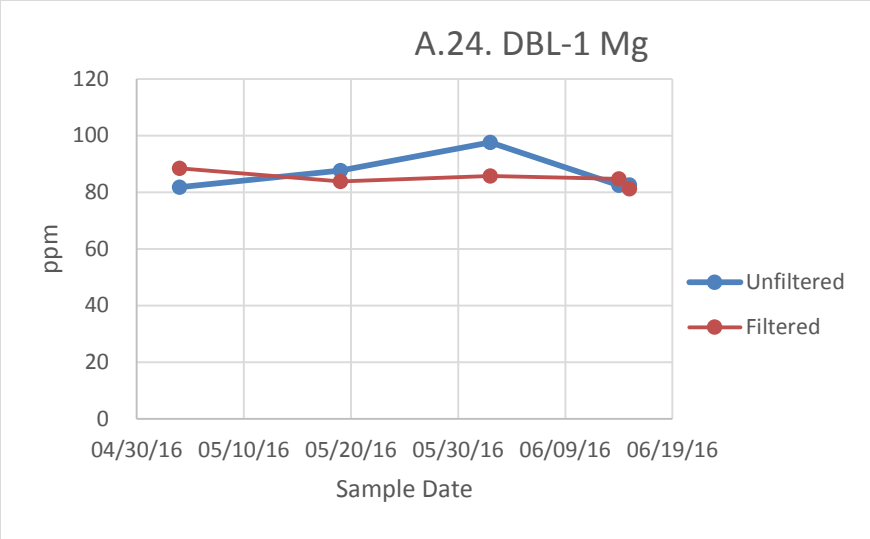
A.24. DBL-1 Mg
120
100
80
60
40
20
0
ppm
04/30/16
05/10/16
05/20/16
05/30/16
06/09/16
06/19/16
Sample Date
Unfiltered
Filtered

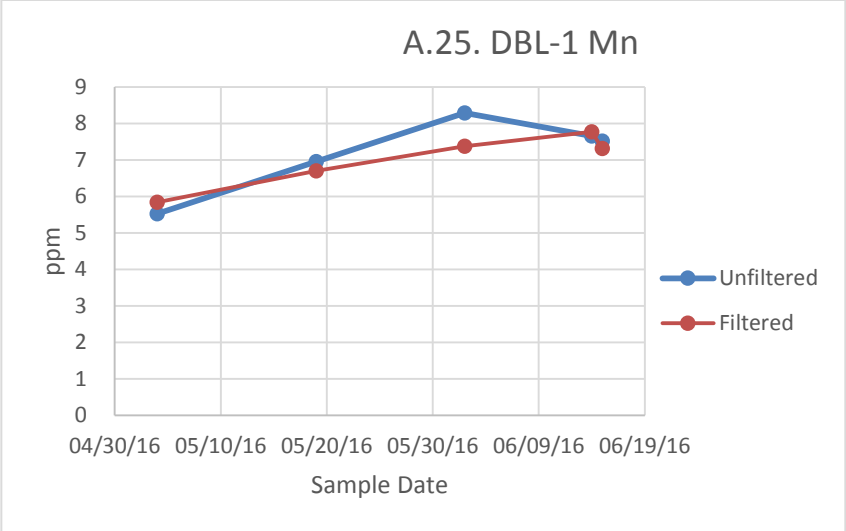
A.25. DBL-1 Mn
9
8
7
6
5
4
3
2
1
0
ppm
04/30/16
05/10/16
05/20/16
05/30/16
06/09/16
06/19/16
Sample Date
Unfiltered
Filtered

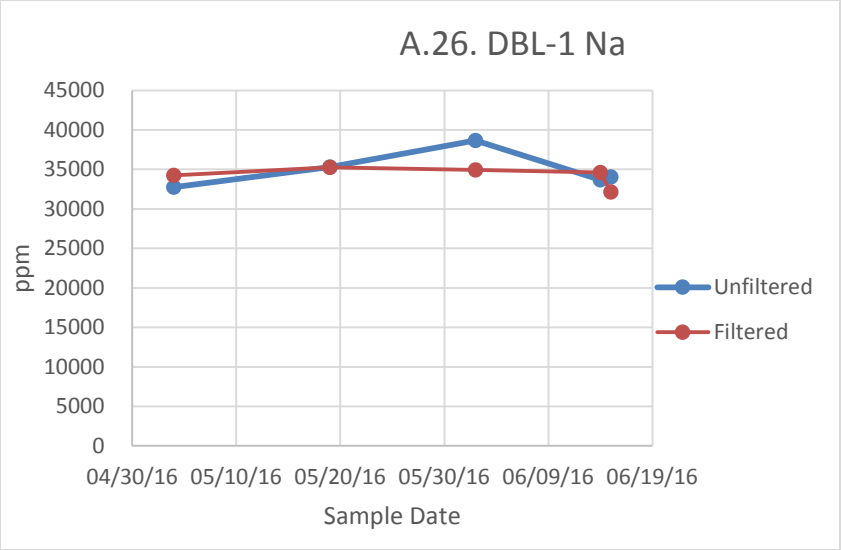
A.26. DBL-1 Na
45000
40000
35000
30000
25000
20000
15000
10000
5000
0
ppm
04/30/16
05/10/16
05/20/16
05/30/16
06/09/16
06/19/16
Sample Date
Unfiltered
Filtered

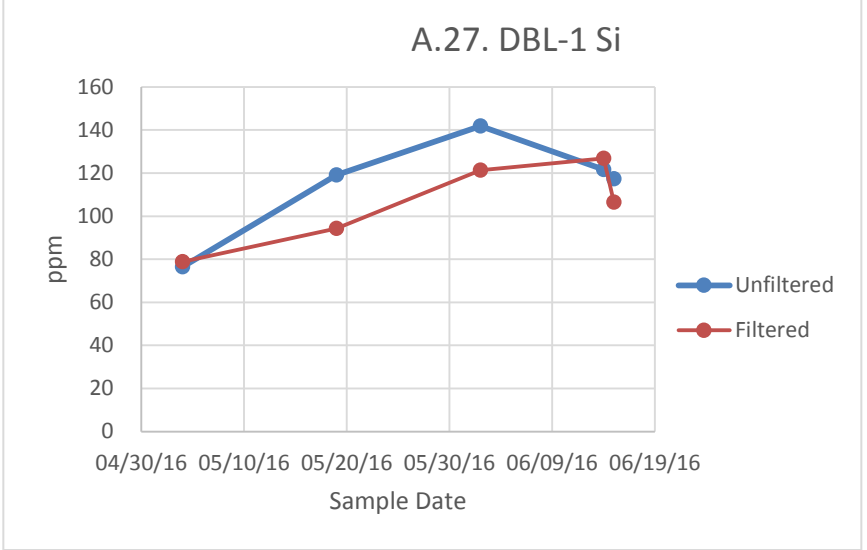
A.27. DBL-1 Si
160
140
120
100
80
60
40
20
0
ppm
04/30/16
05/10/16
05/20/16
05/30/16
06/09/16
06/19/16
Sample Date
Unfiltered
Filtered

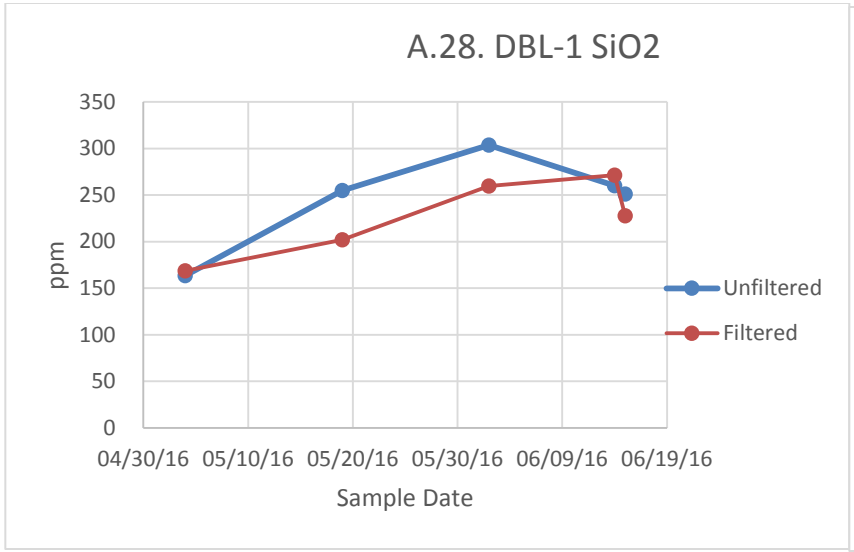
A.28. DBL-1 SiO2
350
300
250
200
150
100
50
0
ppm
04/30/16 05/10/16 05/20/16 05/30/16 06/09/16 06/19/16
Sample Date
Unfiltered
Filtered

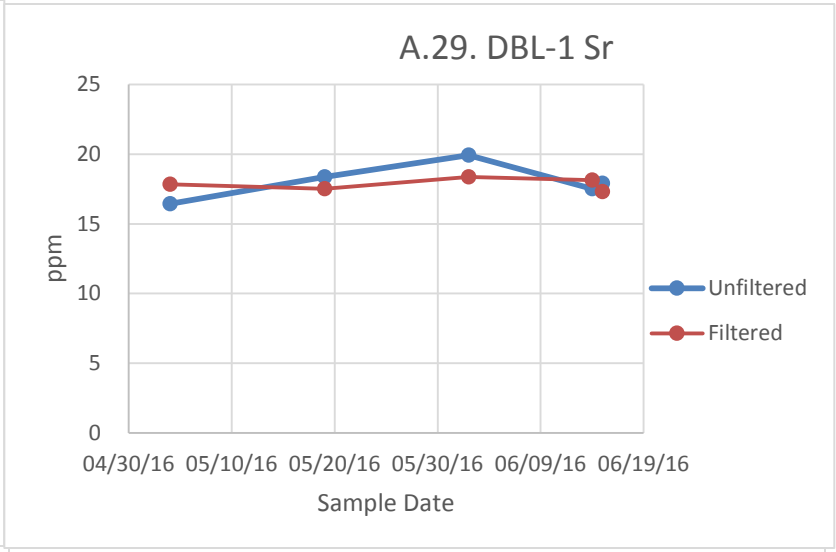
A.29. DBL-1 Sr
25
20
15
10
5
0
ppm
04/30/16 05/10/16 05/20/16 05/30/16 06/09/16 06/19/16
Sample Date
Unfiltered
Filtered

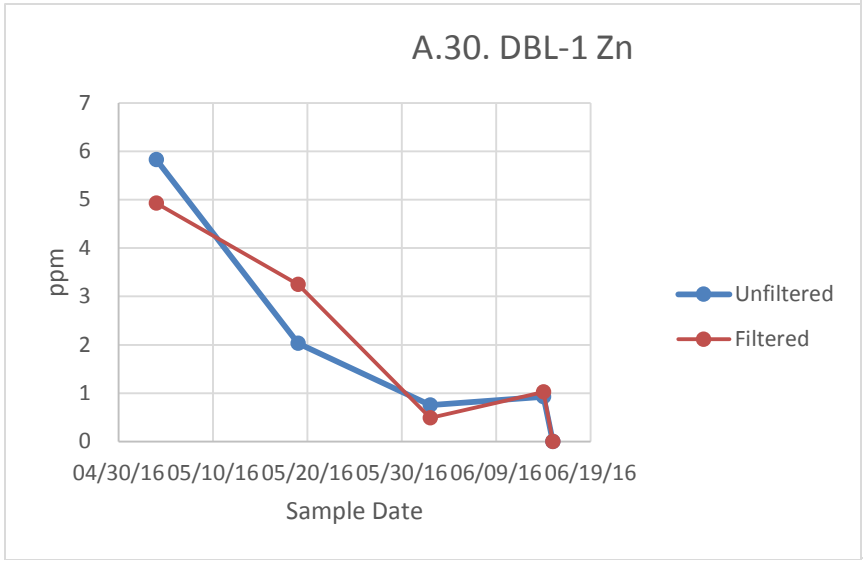
A.30. DBL-1 Zn
7
6
5
4
3
2
1
0
ppm
04/30/16 05/10/16 05/20/16 05/30/16 06/09/16 06/19/16
Sample Date
Unfiltered
Filtered

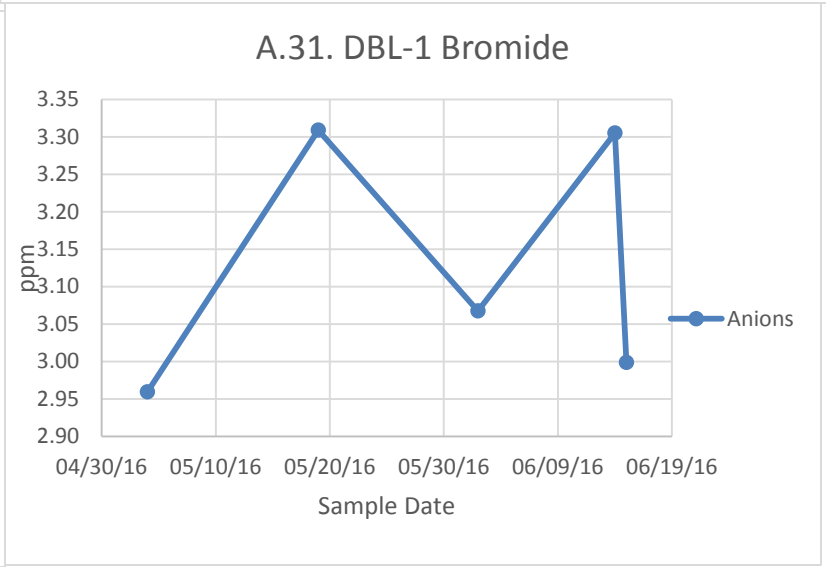
A.31. DBL-1 Bromide
3.35
3.30
3.25
3.20
3.15
3.10
3.05
3.00
2.95
2.90
ppm
04/30/16 05/10/16 05/20/16 05/30/16 06/09/16 06/19/16
Sample Date
Anions

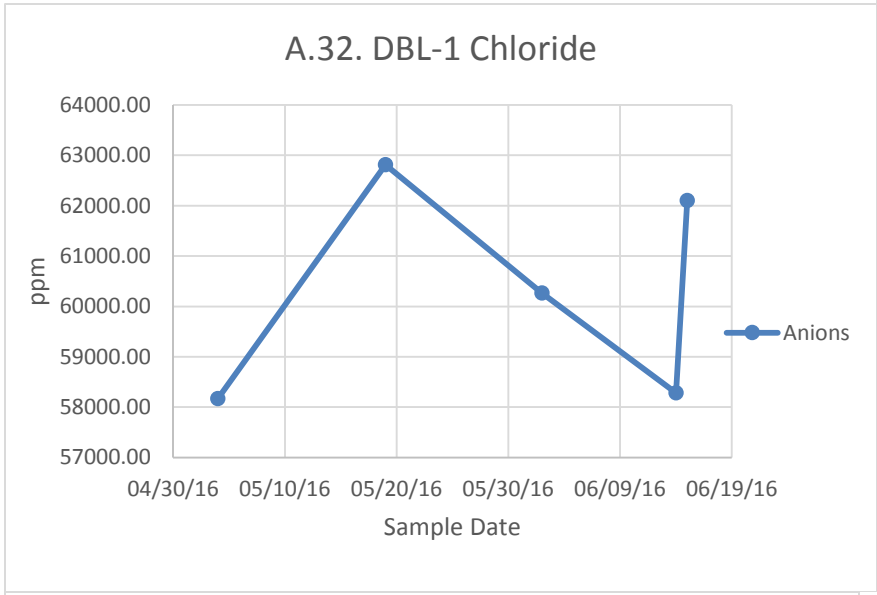
A.32. DBL-1 Chloride
64000.00
63000.00
62000.00
61000.00
60000.00
59000.00
58000.00
57000.00
ppm
04/30/16
05/10/16
05/20/16
05/30/16
06/09/16
06/19/16
Sample Date
Anions

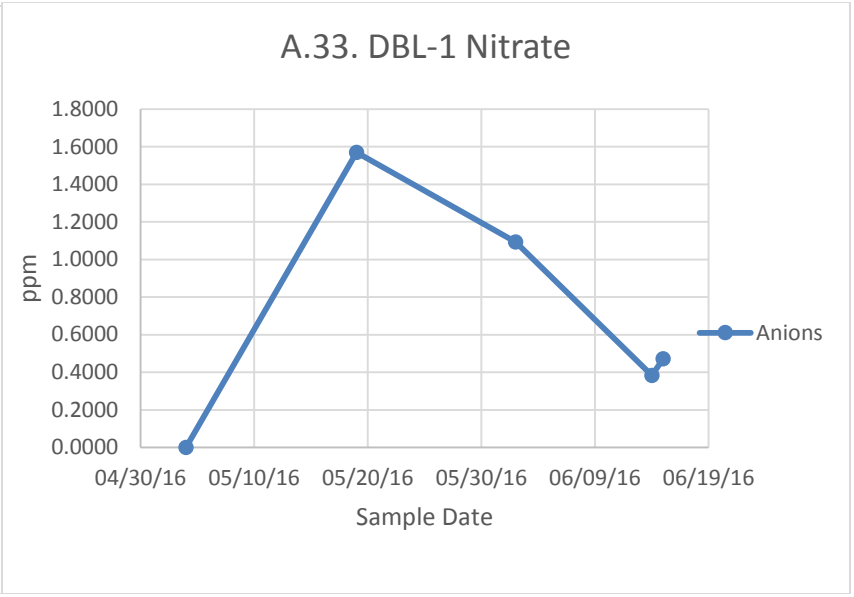
A.33. DBL-1 Nitrate
1.8000
1.6000
1.4000
1.2000
1.0000
0.8000
0.6000
0.4000
0.2000
0.0000
ppm
04/30/16
05/10/16
05/20/16
05/30/16
06/09/16
06/19/16
Sample Date
Anions

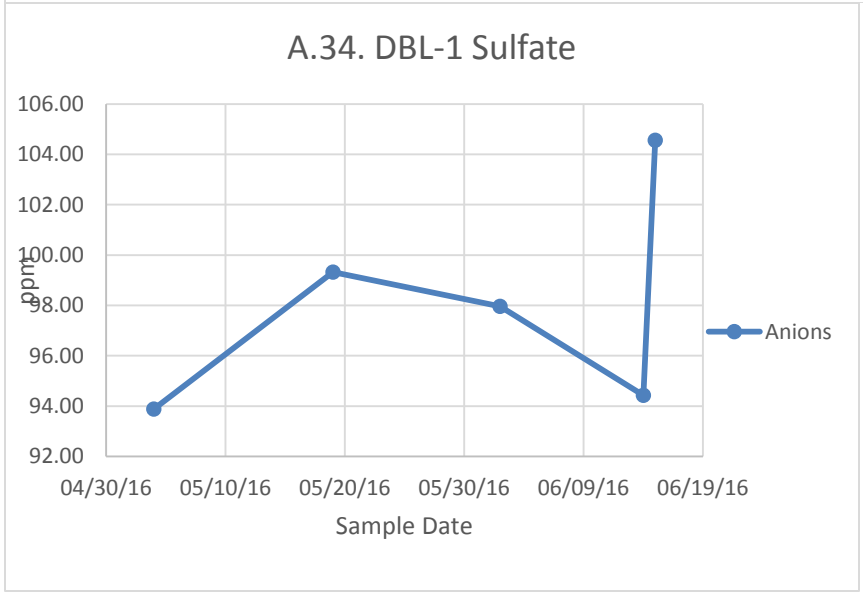
A.34. DBL-1 Sulfate
106.00
104.00
102.00
100.00
98.00
96.00
94.00
92.00
ppm
04/30/16
05/10/16
05/20/16
05/30/16
06/09/16
06/19/16
Sample Date
Anions

APPENDIX B:
Electron Microprobe Standards and Detection Limits

EMP standards and oxide detection limits for silicate analyses

Element	Standard Material	Minimum Detection Limit
Mg	Synthetic Phlogopite	0.02
F	Synthetic Phlogopite	0.11
Na	Albite (Amelia, NC, U.S.A, Rutherford Mine)	0.02
Al	Labradorite (Chihuahua, Mexico)	0.02
Si	Labradorite (Chihuahua, Mexico)	0.02
Ca	Labradorite (Chihuahua, Mexico)	0.01
Cl	Tugtupite (Greenland)	0.01
K	Adularia (St. Gotthard, Switzerland)	0.01
Ti	Titanite glass (Penn State)	0.02
Cr	Synthetic Magnesio-chromite	0.04
Mn	Rhodonite (unknown locality)	0.02
Fe	Augite (unknown locality)	0.02
Ni	Synthetic Liebenbergite	0.06
Zn	Gahnite	0.05
Cs	Pollucite	0.05

[a] Minimum Detection Limit (MDL) values for oxides of respective elements

Appendix C –

Microprobe Analyses of experiments run at 400 ºC, 1 kbar

	Weight Percent													
SAMPLE	**SiO2**	**TiO2**	**Al2O3**	**Cr2O3**	**FeO**	**NiO**	**MnO**	**MgO**	**CaO**	**Na2O**	**K2O**	**Cl**	**F**	**TOTAL**
DBS –1-NaCl														
GREENALITE														
DBS-1 Greenalite -1	28.86	0.00	0.02	0.01	68.29	0.00	0.47	0.61	0.02	0.00	0.01	0.02	0.06	98.36
DBS-1 Greenalite -2	28.83	0.02	0.01	0.01	67.99	0.02	0.46	0.84	0.02	0.01	0.00	0.05	0.00	98.25
Average	**28.85**	**0.01**	**0.02**	**0.01**	**68.14**	**0.01**	**0.46**	**0.73**	**0.02**	**0.00**	**0.00**	**0.03**	**0.03**	**98.30**
Standard Dev.	0.03	0.01	0.00	0.00	0.21	0.01	0.01	0.16	0.00	0.00	0.00	0.02	0.04	0.08
	14 Atoms per formula unit (sum excludes F & Cl)													
	Si	**Ti**	**Al**	**Cr**	**Fe**	**Ni**	**Mn**	**Mg**	**Ca**	**Na**	**K**	**Cl**	**F**	**Sum**
DBS-1 Greenalite - 1	3.477	0.000	0.002	0.001	6.880	0.000	0.048	0.110	0.002	0.000	0.001	0.005	0.021	10.522
DBS-1 Greenalite -2	3.471	0.002	0.002	0.001	6.847	0.002	0.047	0.151	0.003	0.001	0.000	0.009	0.001	10.526
Average	**3.47**	**0.00**	**0.00**	**0.00**	**6.86**	**0.00**	**0.05**	**0.13**	**0.00**	**0.00**	**0.00**	**0.01**	**0.01**	**10.52**
Standard Dev.	0.00	0.00	0.00	0.00	0.02	0.00	0.00	0.03	0.00	0.00	0.00	0.00	0.01	0.00
CHLORITE														
DBS-1 Clay/Chlorite-1	37.99	0.00	11.88	0.00	32.92	0.05	0.05	4.31	0.70	0.49	0.27	1.87	0.27	90.81

DBS-1 Clay/Chlorite-2	35.73	0.02	12.17	0.00	34.85	0.03	0.07	4.10	0.62	0.50	0.24	2.08	0.21	90.61
Average	**36.86**	**0.01**	**12.03**	**0.00**	**33.88**	**0.04**	**0.06**	**4.21**	**0.66**	**0.50**	**0.25**	**1.98**	**0.24**	**90.71**
Standard Dev.	1.60	0.01	0.20	0.00	1.37	0.01	0.01	0.15	0.06	0.00	0.02	0.15	0.04	0.14
	14 Atoms per formula unit (sum excludes F & Cl)													
	Si	**Ti**	**Al**	**Cr**	**Fe**	**Ni**	**Mn**	**Mg**	**Ca**	**Na**	**K**	**Cl**	**F**	**Sum**
DBS-1 Clay/Chlorite-1	4.016	0.000	1.481	0.000	2.910	0.004	0.005	0.679	0.080	0.101	0.036	0.336	0.090	9.312
DBS-1 Clay/Chlorite-2	3.859	0.002	1.549	0.000	3.148	0.002	0.006	0.660	0.072	0.104	0.032	0.381	0.072	9.434
Average	**3.94**	**0.00**	**1.51**	**0.00**	**3.03**	**0.00**	**0.01**	**0.67**	**0.08**	**0.10**	**0.03**	**0.36**	**0.08**	**9.37**
Standard Dev.	0.11	0.00	0.05	0.00	0.17	0.00	0.00	0.01	0.01	0.00	0.00	0.03	0.01	0.09
PLAG														
DBS-1 Plag -1	66.91	0.01	24.14	0.00	0.26	0.00	0.00	0.01	4.55	8.27	1.03	0.01	0.00	105.19
DBS-1 Plag -2	68.74	0.02	24.83	0.00	0.23	0.00	0.00	0.01	4.70	6.32	0.97	0.01	0.02	105.86
Average	**67.82**	**0.02**	**24.49**	**0.00**	**0.24**	**0.00**	**0.00**	**0.01**	**4.63**	**7.29**	**1.00**	**0.01**	**0.01**	**105.53**
Standard Dev.	1.29	0.00	0.49	0.00	0.02	0.00	0.00	0.01	0.11	1.38	0.04	0.00	0.01	0.48
	8 Atoms per formula unit (sum excludes F & Cl)													
	Si	**Ti**	**Al**	**Cr**	**Fe**	**Ni**	**Mn**	**Mg**	**Ca**	**Na**	**K**	**Cl**	**F**	**Sum**
DBS-1 Plag-1	2.813	0.000	1.196	0.000	0.009	0.000	0.000	0.000	0.205	0.674	0.055	0.001	0.001	4.953
DBS-1 Plag -2	2.843	0.001	1.211	0.000	0.008	0.000	0.000	0.001	0.208	0.507	0.051	0.001	0.003	4.830
Average	**2.83**	**0.00**	**1.20**	**0.00**	**0.01**	**0.00**	**0.00**	**0.00**	**0.21**	**0.59**	**0.05**	**0.00**	**0.00**	**4.89**
Standard Dev.	0.02	0.00	0.01	0.00	0.00	0.00	0.00	0.00	0.00	0.12	0.00	0.00	0.00	0.09

DB-12 -CaCl														
OPX - Ferrosilite														
DB-12 Pyroxene -1	49.90	0.03	1.24	0.43	35.79	0.07	0.21	10.02	4.03	0.03	0.00	0.04	0.07	101.84
DB-12 Pyroxene -2	49.70	0.04	2.47	0.47	31.47	0.06	0.18	10.61	6.06	0.04	0.00	0.05	0.00	101.15
Average	**49.80**	**0.03**	**1.86**	**0.45**	**33.63**	**0.06**	**0.19**	**10.31**	**5.04**	**0.04**	**0.00**	**0.04**	**0.03**	**101.50**
Standard Dev.	0.14	0.00	0.87	0.03	3.06	0.00	0.02	0.42	1.44	0.01	0.00	0.01	0.05	0.49
	6 Atoms per formula unit (sum excludes F & Cl)													
	Si	**Ti**	**Al**	**Cr**	**Fe**	**Ni**	**Mn**	**Mg**	**Ca**	**Na**	**K**	**Cl**	**F**	**Sum**
DB-12 Pyroxene -1	1.970	0.001	0.058	0.013	1.182	0.002	0.007	0.590	0.170	0.002	0.000	0.003	0.008	3.995
DB-12 Pyroxene -2	1.946	0.001	0.114	0.015	1.030	0.002	0.006	0.619	0.254	0.003	0.000	0.003	0.000	3.991
Average	**1.96**	**0.00**	**0.09**	**0.01**	**1.11**	**0.00**	**0.01**	**0.60**	**0.21**	**0.00**	**0.00**	**0.00**	**0.00**	**3.99**
Standard Dev.	0.02	0.00	0.04	0.00	0.11	0.00	0.00	0.02	0.06	0.00	0.00	0.00	0.01	0.00
CLINOZOISITE														
DB-12 CZO -1	47.14	0.01	34.26	0.01	0.52	0.03	0.00	0.02	17.70	1.13	0.02	0.06	0.04	100.93
DB-12 CZO -1	47.32	0.00	34.71	0.00	0.44	0.01	0.00	0.00	17.59	1.14	0.03	0.55	0.04	101.84
DB-12 CZO -1	44.76	0.00	35.50	0.00	0.67	0.09	0.00	0.03	17.80	0.85	0.02	0.39	0.00	100.12
Average	**46.41**	**0.00**	**34.82**	**0.00**	**0.54**	**0.04**	**0.00**	**0.01**	**17.70**	**1.04**	**0.02**	**0.33**	**0.03**	**100.96**
Standard Dev.	1.43	0.01	0.63	0.00	0.12	0.04	0.00	0.01	0.10	0.16	0.01	0.25	0.02	0.86
	12.5 Atoms per formula unit (sum excludes F & Cl)													
	Si	**Ti**	**Al**	**Cr**	**Fe**	**Ni**	**Mn**	**Mg**	**Ca**	**Na**	**K**	**Cl**	**F**	**Sum**
DB-12 CZO -1	3.359	0.001	2.877	0.000	0.031	0.001	0.000	0.002	1.352	0.156	0.002	0.007	0.010	7.781
DB-12 CZO -1	3.354	0.000	2.899	0.000	0.026	0.001	0.000	0.000	1.336	0.157	0.003	0.066	0.009	7.776
DB-12 CZO -1	3.237	0.000	3.025	0.000	0.041	0.005	0.000	0.003	1.379	0.119	0.002	0.048	0.000	7.811
Average	**3.32**	**0.00**	**2.93**	**0.00**	**0.03**	**0.00**	**0.00**	**0.00**	**1.36**	**0.14**	**0.00**	**0.04**	**0.01**	**7.79**
Standard Dev.	0.07	0.00	0.08	0.00	0.01	0.00	0.00	0.00	0.02	0.02	0.00	0.03	0.01	0.02

WAIRAKITE														
DB-12 WAIR -1	73.59	0.03	16.36	0.00	0.49	0.00	0.01	0.04	9.06	0.45	0.01	0.05	0.04	100.13
DB-12 WAIR -2	65.01	0.03	23.60	0.00	0.46	0.02	0.00	0.03	11.71	0.64	0.00	0.11	0.12	101.73
Average	**69.30**	**0.03**	**19.98**	**0.00**	**0.47**	**0.01**	**0.01**	**0.03**	**10.39**	**0.54**	**0.00**	**0.08**	**0.08**	**100.93**
Standard Dev.	6.07	0.00	5.11	0.00	0.02	0.01	0.01	0.01	1.88	0.14	0.00	0.04	0.06	1.14
	12 Atoms per formula unit (sum excludes F & Cl)													
	Si	**Ti**	**Al**	**Cr**	**Fe**	**Ni**	**Mn**	**Mg**	**Ca**	**Na**	**K**	**Cl**	**F**	**Sum**
DB-12 WAIR -1	4.728	0.002	1.239	0.000	0.026	0.000	0.001	0.004	0.624	0.055	0.001	0.005	0.008	6.679
DB-12 WAIR -2	4.208	0.002	1.800	0.000	0.025	0.001	0.000	0.003	0.812	0.081	0.000	0.012	0.025	6.931
Average	**4.47**	**0.00**	**1.52**	**0.00**	**0.03**	**0.00**	**0.00**	**0.00**	**0.72**	**0.07**	**0.00**	**0.01**	**0.02**	**6.80**
Standard Dev.	0.37	0.00	0.40	0.00	0.00	0.00	0.00	0.00	0.13	0.02	0.00	0.00	0.01	0.18
AMPHIBOLE / FERROHASTINGITE														
DB-12 Ferro -1	48.26	0.25	1.46	0.01	34.58	0.06	0.19	10.94	3.04	0.00	0.00	0.12	0.00	98.91
DB-12 Ferro -2	48.45	0.16	1.10	0.01	36.16	0.05	0.16	10.39	2.72	0.00	0.01	0.03	0.00	99.23
DB-12 Ferro -3	48.20	0.27	1.66	0.02	31.90	0.04	0.19	10.73	5.10	0.03	0.00	0.02	0.00	98.15
DB-12 Ferro -1	48.72	0.16	1.41	0.02	35.65	0.03	0.15	10.30	3.09	0.04	0.00	0.00	0.03	99.61
DB-12 Ferro -2	48.19	0.26	2.60	0.00	32.51	0.06	0.18	9.35	6.24	0.01	0.01	0.25	0.00	99.66
Average	**48.36**	**0.22**	**1.65**	**0.01**	**34.16**	**0.05**	**0.17**	**10.34**	**4.04**	**0.02**	**0.00**	**0.08**	**0.01**	**99.11**
Standard Dev.	0.23	0.06	0.57	0.01	1.89	0.01	0.02	0.61	1.55	0.02	0.00	0.10	0.02	0.62
	22 Atoms per formula unit (sum excludes F & Cl)													
	Si	**Ti**	**Al**	**Cr**	**Fe**	**Ni**	**Mn**	**Mg**	**Ca**	**Na**	**K**	**Cl**	**F**	**Sum**
DB-12 Ferro -1	7.165	0.028	0.255	0.001	4.294	0.007	0.023	2.422	0.484	0.000	0.000	0.030	0.000	14.680
DB-12 Ferro -2	7.206	0.018	0.193	0.001	4.498	0.006	0.020	2.304	0.433	0.001	0.001	0.007	0.000	14.681
DB-12 Ferro -3	7.159	0.030	0.291	0.003	3.962	0.005	0.023	2.375	0.812	0.008	0.000	0.005	0.000	14.668

DB-12 Ferro -1	7.201	0.017	0.246	0.002	4.406	0.003	0.019	2.269	0.489	0.012	0.000	0.001	0.016	14.664
DB-12 Ferro -2	7.096	0.029	0.451	0.000	4.005	0.008	0.023	2.053	0.984	0.002	0.001	0.063	0.000	14.651
Average	**7.17**	**0.02**	**0.29**	**0.00**	**4.23**	**0.01**	**0.02**	**2.28**	**0.64**	**0.00**	**0.00**	**0.02**	**0.00**	**14.67**
Standard Dev.	0.04	0.01	0.10	0.00	0.24	0.00	0.00	0.14	0.24	0.01	0.00	0.03	0.01	0.01
CHLORITE														
DB-12 Chl-1	26.87	0.07	18.37	0.01	35.15	1.01	0.16	4.10	1.19	0.48	0.07	2.52	0.09	90.08
DB-12 Chl-2	27.59	0.04	19.49	0.00	35.89	0.31	0.13	4.62	0.97	0.09	0.06	1.01	0.07	90.28
DB-12 Chl-1	27.46	0.04	19.20	0.00	36.32	0.32	0.13	4.47	1.05	0.06	0.09	1.07	0.12	90.32
DB-12 Chl-2	29.28	0.02	20.61	0.00	36.20	0.46	0.14	4.49	1.19	0.10	0.09	1.14	0.04	93.76
DB-12 Chl-1	25.69	0.04	18.19	0.00	33.57	1.17	0.23	4.11	1.42	0.51	0.12	3.27	0.04	88.36
Average	**27.38**	**0.04**	**19.17**	**0.00**	**35.43**	**0.65**	**0.16**	**4.36**	**1.16**	**0.25**	**0.09**	**1.80**	**0.07**	**90.56**
Standard Dev.	1.30	0.02	0.97	0.01	1.13	0.41	0.04	0.24	0.17	0.23	0.02	1.03	0.03	1.97
	14 Atoms per formula unit (sum excludes F & Cl)													
	Si	**Ti**	**Al**	**Cr**	**Fe**	**Ni**	**Mn**	**Mg**	**Ca**	**Na**	**K**	**Cl**	**F**	**Sum**
DB-12 Chl-1	3.020	0.006	2.433	0.001	3.304	0.091	0.015	0.687	0.143	0.105	0.010	0.479	0.030	9.814
DB-12 Chl-2	3.015	0.004	2.510	0.000	3.279	0.027	0.012	0.752	0.114	0.019	0.009	0.187	0.025	9.740
DB-12 Chl-1	3.013	0.003	2.483	0.000	3.334	0.028	0.013	0.731	0.123	0.012	0.013	0.199	0.042	9.754
DB-12 Chl-2	3.061	0.002	2.540	0.000	3.165	0.038	0.012	0.700	0.133	0.020	0.012	0.203	0.012	9.684
DB-12 Chl-1	2.972	0.004	2.480	0.000	3.248	0.108	0.022	0.709	0.176	0.114	0.018	0.642	0.016	9.851
Average	**3.02**	**0.00**	**2.49**	**0.00**	**3.27**	**0.06**	**0.01**	**0.72**	**0.14**	**0.05**	**0.01**	**0.34**	**0.03**	**9.77**
Standard Dev.	0.03	0.00	0.04	0.00	0.06	0.04	0.00	0.03	0.02	0.05	0.00	0.21	0.01	0.07

	Weight Percent														
SAMPLE	SiO_2	TiO_2	Al_2O_3	Cr_2O_3	FeO	NiO	MnO	MgO	CaO	Na_2O	K_2O	Cs_2O	Cl	F	TOTAL
DBS -17 – Cs/Ca/NaCl															
Pollucite-Wairakite															
DBS-17 Pol -1	58.49	0.00	19.40	0.00	0.37	0.02	0.00	0.02	4.92	1.28	0.05	13.49	0.19	0.01	98.24
DBS-17 Pol -2	56.45	0.00	19.05	0.02	0.71	0.00	0.01	0.07	5.59	1.06	0.05	11.37	0.34	0.05	94.77
DBS-17 Pol -3	47.83	0.00	19.79	0.00	0.42	0.03	0.03	0.02	4.60	1.53	0.04	13.72	0.14	0.01	88.15
DBS-17 Pol -4	56.79	0.00	18.90	0.03	0.31	0.00	0.00	0.00	4.67	1.33	0.03	14.53	0.10	0.00	96.68
DBS-17 Pol -5	54.12	0.00	18.34	0.01	0.29	0.00	0.00	0.00	4.33	1.20	0.03	14.72	0.16	0.00	93.21
DBS-17 Pol -6	58.66	0.00	18.56	0.00	0.28	0.00	0.02	0.00	4.82	1.26	0.04	14.46	0.08	0.01	98.19
DBS-17 Pol -7	55.78	0.00	19.27	0.00	1.07	0.01	0.00	0.10	5.19	1.29	0.04	12.41	0.29	0.00	95.45
DBS-17 Pol -8	58.96	0.00	18.38	0.00	0.25	0.00	0.04	0.00	4.63	1.35	0.04	15.53	0.03	0.00	99.20
DBS-17 Pol -9	56.46	0.00	17.72	0.01	0.24	0.00	0.01	0.00	4.49	1.19	0.03	16.04	0.04	0.02	96.25
DBS-17 Pol -10	56.65	0.00	18.92	0.00	0.56	0.00	0.00	0.03	4.61	1.30	0.03	14.99	0.04	0.04	97.19
DBS-17 Pol -11	54.99	0.00	18.15	0.01	0.26	0.00	0.02	0.00	4.26	1.24	0.02	15.73	0.33	0.00	95.02
DBS-17 Pol -12	57.76	0.00	18.16	0.00	0.27	0.00	0.02	0.00	4.48	1.27	0.04	14.94	0.09	0.00	97.03
DBS-17 Pol -13	55.76	0.00	17.68	0.00	0.28	0.00	0.03	0.00	4.68	1.27	0.03	15.51	0.03	0.00	95.28
DBS-17 Pol -14	57.67	0.00	18.79	0.02	0.45	0.01	0.01	0.04	5.20	1.17	0.03	11.67	0.25	0.01	95.32
DBS-17 Pol -15	57.51	0.00	19.30	0.00	0.71	0.00	0.01	0.08	5.71	1.27	0.02	12.03	0.16	0.02	96.81
DBS-17 Pol -16	60.08	0.00	15.85	0.02	2.35	0.03	0.02	0.25	3.99	1.22	0.22	10.19	0.34	0.02	94.57
DBS-17 Pol -17	58.55	0.00	16.92	0.00	1.55	0.00	0.01	0.16	4.71	1.29	0.06	11.59	0.21	0.00	95.07
DBS-17 Pol -18	55.03	0.00	20.67	0.00	1.49	0.00	0.02	0.16	6.05	1.11	0.04	12.71	0.25	0.03	97.55
DBS-17 Pol -19	58.21	0.00	18.76	0.00	0.84	0.00	0.02	0.07	5.03	1.84	0.05	12.81	1.00	0.04	98.69
DBS-17 Pol -20	56.42	0.00	18.89	0.00	1.02	0.00	0.02	0.07	5.64	1.18	0.06	12.51	0.23	0.00	96.04
DBS-17 Pol -21	58.43	0.00	18.13	0.00	0.35	0.00	0.00	0.00	4.71	1.23	0.03	14.49	0.04	0.00	97.42
DBS-17 Pol -22	58.39	0.00	17.96	0.02	0.27	0.00	0.02	0.00	4.46	1.23	0.04	16.54	0.03	0.00	98.96
DBS-17 Pol -23	55.92	0.00	20.14	0.01	1.06	0.03	0.00	0.12	5.81	1.16	0.05	11.90	0.32	0.02	96.53

DBS-17 Pol -24	57.53	0.00	19.57	0.00	0.66	0.00	0.03	0.04	5.10	1.33	0.03	13.34	0.07	0.00	97.70
DBS-17 Pol -25	53.65	0.00	18.42	0.00	0.97	0.00	0.01	0.08	5.81	1.21	0.03	11.70	0.25	0.00	92.14
Average	**56.64**	**0.00**	**18.63**	**0.01**	**0.68**	**0.01**	**0.01**	**0.05**	**4.94**	**1.27**	**0.05**	**13.56**	**0.20**	**0.01**	**96.06**
Std Dev	2.43	0.00	1.01	0.01	0.52	0.01	0.01	0.06	0.55	0.15	0.04	1.72	0.20	0.02	2.40
	6 Oxygen Basis Atoms per Formula Unit (sum excludes F & Cl)														
	Si	**Ti**	**Al**	**Cr**	**Fe**	**Ni**	**Mn**	**Mg**	**Ca**	**Na**	**K**	**Cs**	**Cl**	**F**	**Sum**
DBS-17 Pol -1	2.179	0.000	0.852	0.000	0.011	0.000	0.000	0.001	0.197	0.093	0.002	0.214	0.012	0.002	3.550
DBS-17 Pol -2	2.160	0.000	0.859	0.001	0.023	0.000	0.000	0.004	0.229	0.078	0.002	0.185	0.022	0.006	3.543
DBS-17 Pol -3	2.043	0.000	0.997	0.000	0.015	0.001	0.001	0.002	0.211	0.127	0.002	0.250	0.010	0.001	3.648
DBS-17 Pol -4	2.174	0.000	0.853	0.001	0.010	0.000	0.000	0.000	0.192	0.099	0.001	0.237	0.006	0.000	3.567
DBS-17 Pol -5	2.167	0.000	0.865	0.000	0.010	0.000	0.000	0.000	0.186	0.093	0.002	0.251	0.011	0.000	3.574
DBS-17 Pol -6	2.201	0.000	0.821	0.000	0.009	0.000	0.001	0.000	0.194	0.091	0.002	0.231	0.005	0.001	3.550
DBS-17 Pol -7	2.143	0.000	0.873	0.000	0.034	0.000	0.000	0.006	0.214	0.096	0.002	0.203	0.019	0.000	3.571
DBS-17 Pol -8	2.207	0.000	0.811	0.000	0.008	0.000	0.001	0.000	0.186	0.098	0.002	0.248	0.002	0.000	3.561
DBS-17 Pol -9	2.202	0.000	0.814	0.000	0.008	0.000	0.000	0.000	0.188	0.090	0.002	0.267	0.002	0.002	3.570
DBS-17 Pol -10	2.169	0.000	0.854	0.000	0.018	0.000	0.000	0.002	0.189	0.096	0.002	0.245	0.003	0.005	3.575
DBS-17 Pol -11	2.179	0.000	0.848	0.000	0.009	0.000	0.001	0.000	0.181	0.095	0.001	0.266	0.022	0.000	3.579
DBS-17 Pol -12	2.206	0.000	0.817	0.000	0.009	0.000	0.001	0.000	0.183	0.094	0.002	0.243	0.006	0.000	3.555
DBS-17 Pol -13	2.192	0.000	0.819	0.000	0.009	0.000	0.001	0.000	0.197	0.097	0.001	0.260	0.002	0.000	3.577
DBS-17 Pol -14	2.187	0.000	0.840	0.001	0.014	0.000	0.000	0.002	0.211	0.086	0.001	0.189	0.016	0.001	3.531
DBS-17 Pol -15	2.160	0.000	0.854	0.000	0.022	0.000	0.000	0.005	0.230	0.093	0.001	0.193	0.010	0.002	3.557
DBS-17 Pol -16	2.277	0.000	0.708	0.001	0.075	0.001	0.001	0.014	0.162	0.089	0.010	0.165	0.022	0.003	3.501
DBS-17 Pol -17	2.232	0.000	0.760	0.000	0.049	0.000	0.000	0.009	0.192	0.096	0.003	0.189	0.014	0.000	3.531
DBS-17 Pol -18	2.085	0.000	0.923	0.000	0.047	0.000	0.001	0.009	0.246	0.081	0.002	0.205	0.016	0.004	3.598
DBS-17 Pol -19	2.178	0.000	0.827	0.000	0.026	0.000	0.001	0.004	0.202	0.134	0.003	0.204	0.063	0.005	3.579
DBS-17 Pol -20	2.155	0.000	0.850	0.000	0.033	0.000	0.001	0.004	0.231	0.087	0.003	0.204	0.015	0.000	3.567
DBS-17 Pol -21	2.211	0.000	0.809	0.000	0.011	0.000	0.000	0.000	0.191	0.090	0.002	0.234	0.002	0.000	3.548
DBS-17 Pol -22	2.213	0.000	0.802	0.001	0.009	0.000	0.000	0.000	0.181	0.091	0.002	0.267	0.002	0.000	3.566

DBS-17 Pol -23	2.117	0.000	0.899	0.000	0.034	0.001	0.000	0.007	0.236	0.085	0.003	0.192	0.020	0.003	3.573
DBS-17 Pol -24	2.158	0.000	0.865	0.000	0.021	0.000	0.001	0.002	0.205	0.097	0.002	0.213	0.004	0.000	3.565
DBS-17 Pol -25	2.136	0.000	0.864	0.000	0.032	0.000	0.000	0.005	0.248	0.093	0.001	0.199	0.017	0.000	3.579
Average	**2.173**	**0.000**	**0.843**	**0.000**	**0.022**	**0.000**	**0.000**	**0.003**	**0.203**	**0.095**	**0.002**	**0.222**	**0.013**	**0.001**	**3.565**
Std Dev	0.047	0.000	0.053	0.000	0.017	0.000	0.000	0.004	0.022	0.012	0.002	0.030	0.013	0.002	0.026
DBS-17: (dense clay)															
DBS-17 Mica -1	34.04	0.00	18.45	0.00	11.88	0.00	0.07	1.49	2.07	0.16	0.22	7.87	1.81	0.17	78.25
DBS-17 Mica -3	28.54	0.00	13.42	0.01	15.59	0.01	0.10	1.67	3.34	0.34	0.22	8.81	3.98	0.02	76.06
DBS-17 Mica -4	39.87	0.00	10.05	0.00	12.68	0.00	0.08	1.42	2.22	0.18	0.18	7.91	2.27	0.05	76.91
Average	**34.15**	**0.00**	**13.97**	**0.00**	**13.38**	**0.00**	**0.09**	**1.53**	**2.54**	**0.23**	**0.21**	**8.20**	**2.69**	**0.08**	**77.07**
Std Dev	5.67	0.00	4.23	0.01	1.95	0.01	0.01	0.13	0.69	0.10	0.02	0.53	1.14	0.08	1.11
Fe-rich clay															
DBS-17 Mica	25.29	0.00	12.67	0.00	20.55	0.00	0.08	1.95	1.65	0.81	0.20	11.72	3.63	0.13	78.68
	6 Oxygen Basis Atoms per Formula Unit (sum excludes F & Cl)														
	Si	**Ti**	**Al**	**Cr**	**Fe**	**Ni**	**Mn**	**Mg**	**Ca**	**Na**	**K**	**Cs**	**Cl**	**F**	**Sum**
DBS-17 Mica -1	1.744	0.000	1.114	0.000	0.509	0.000	0.003	0.114	0.114	0.016	0.015	0.172	0.158	0.028	3.800
DBS-17 Mica -3	1.673	0.000	0.927	0.001	0.764	0.000	0.005	0.146	0.210	0.039	0.016	0.220	0.395	0.004	4.001
DBS-17 Mica -4	2.087	0.000	0.620	0.000	0.555	0.000	0.004	0.111	0.124	0.018	0.012	0.176	0.201	0.009	3.707
Average	**1.834**	**0.000**	**0.887**	**0.000**	**0.609**	**0.000**	**0.004**	**0.123**	**0.149**	**0.025**	**0.014**	**0.190**	**0.251**	**0.014**	**3.836**
Std Dev	0.221	0.000	0.249	0.000	0.136	0.000	0.001	0.020	0.053	0.013	0.002	0.027	0.126	0.013	0.151
Fe-rich clay															
DBS-17 Mica -2	1.543	0.000	0.912	0.000	1.049	0.000	0.004	0.177	0.108	0.096	0.016	0.305	0.376	0.025	4.209

Appendix D

XRD mineral analyses and quantification. Experiments run at 400 ºC, 1 kbar

	Wyoming Bentonite starting material	8. 9. DBS NaCl	DBS CaCl	DBS Cs/Na/CaCl
		Two Weeks 400°C 1Kbar		
Smectite	72			
Chlorite	b.d.l.		31.7	31.7
Kaolinite	b.d.l.	5		
Clinoptilolite	13			
Analcime / Wairakite	b.d.l.		2	5.9
Pollucite				14.9
Quartz	1	25		
Cristobalite/ Opal-C	2			
Biotite	3			
Pyrite	0.4			
Plagioclase	9	64	26.7	17.8
K-Feldspar	b.d.l.			
Ferrosilite			22.6	15.8
Calcite	6			
Dolomite	+			
Siderite	2			
Halite		5		
Clinozoisite			17.8	13.9
Total:	100.4	99	98.8	100

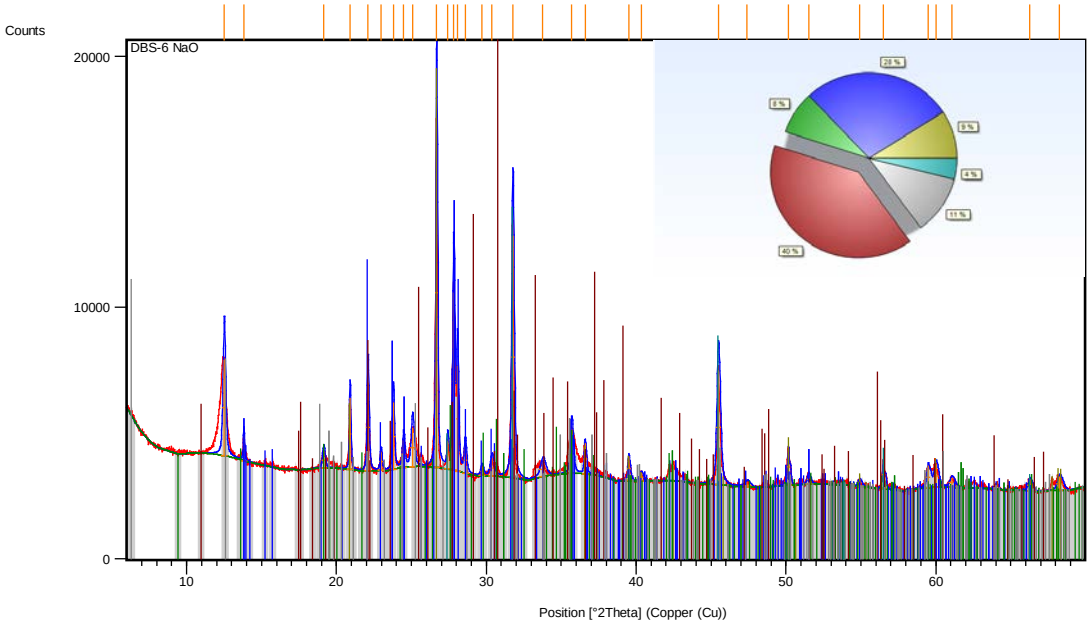

XRD Spectra analysis of DBS-6 (NaCl run)

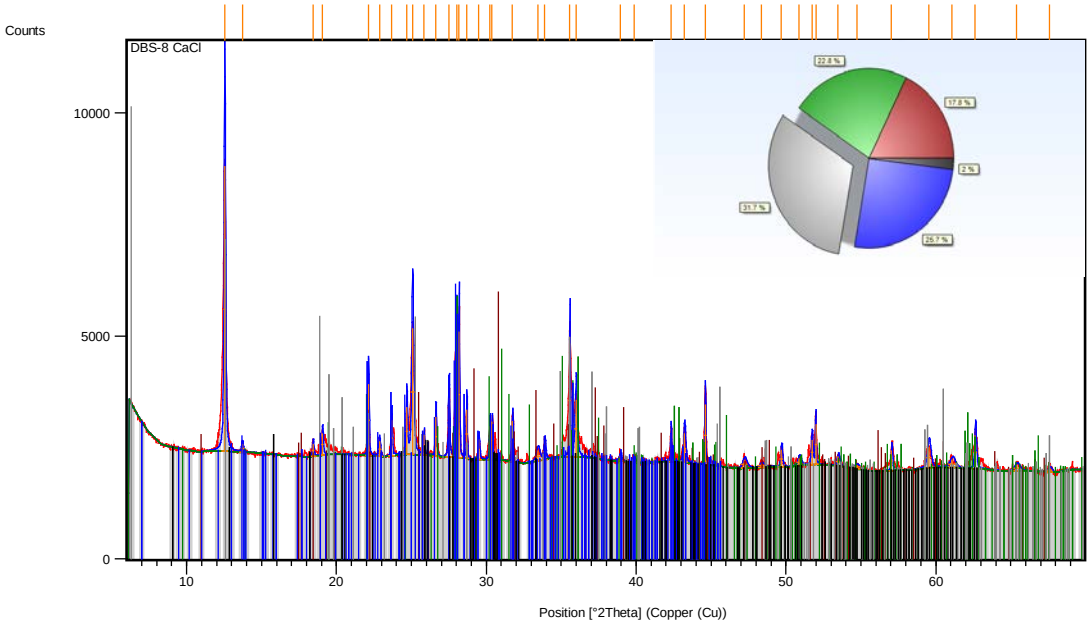

XRD Spectra analysis of DBS-8 (CaCl run)

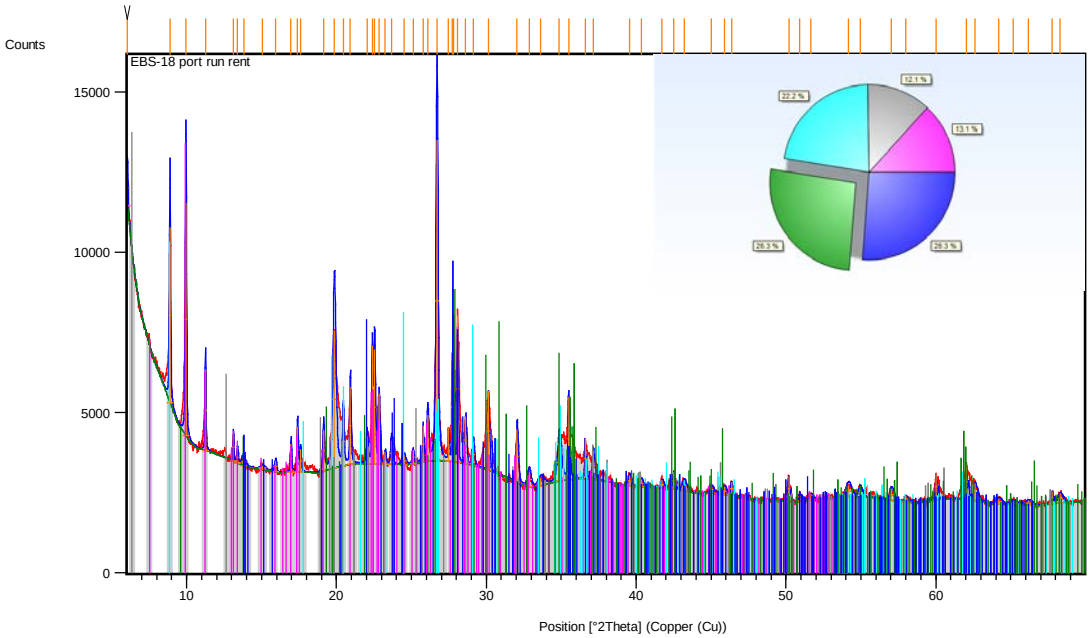

XRD Spectra analysis of DBS-18 (Cs/Ca/NaCl run)

Appendix E

SEM images

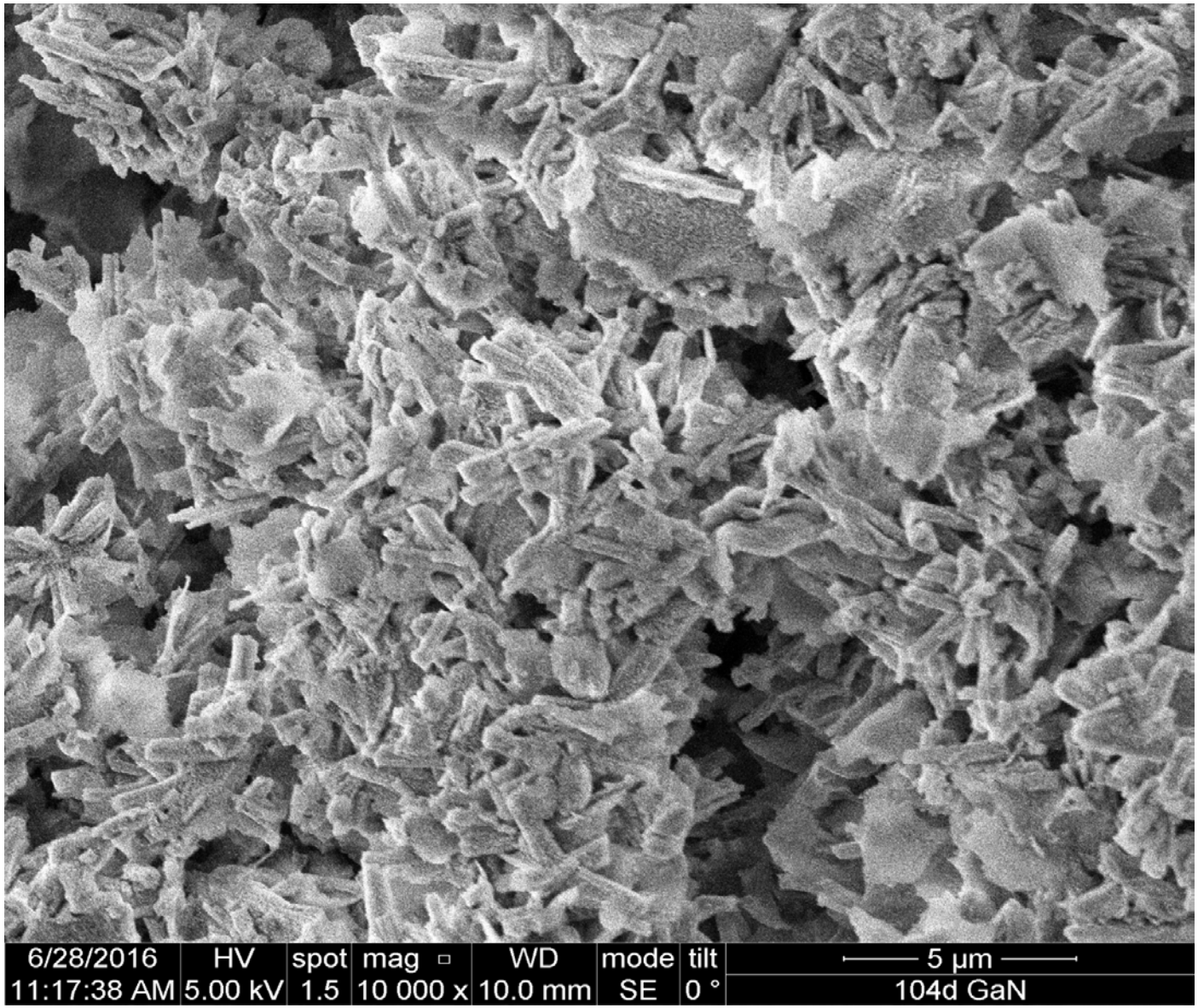

Figure E.1. Chlorite sprays in sample DBS21 (NaCl brine)

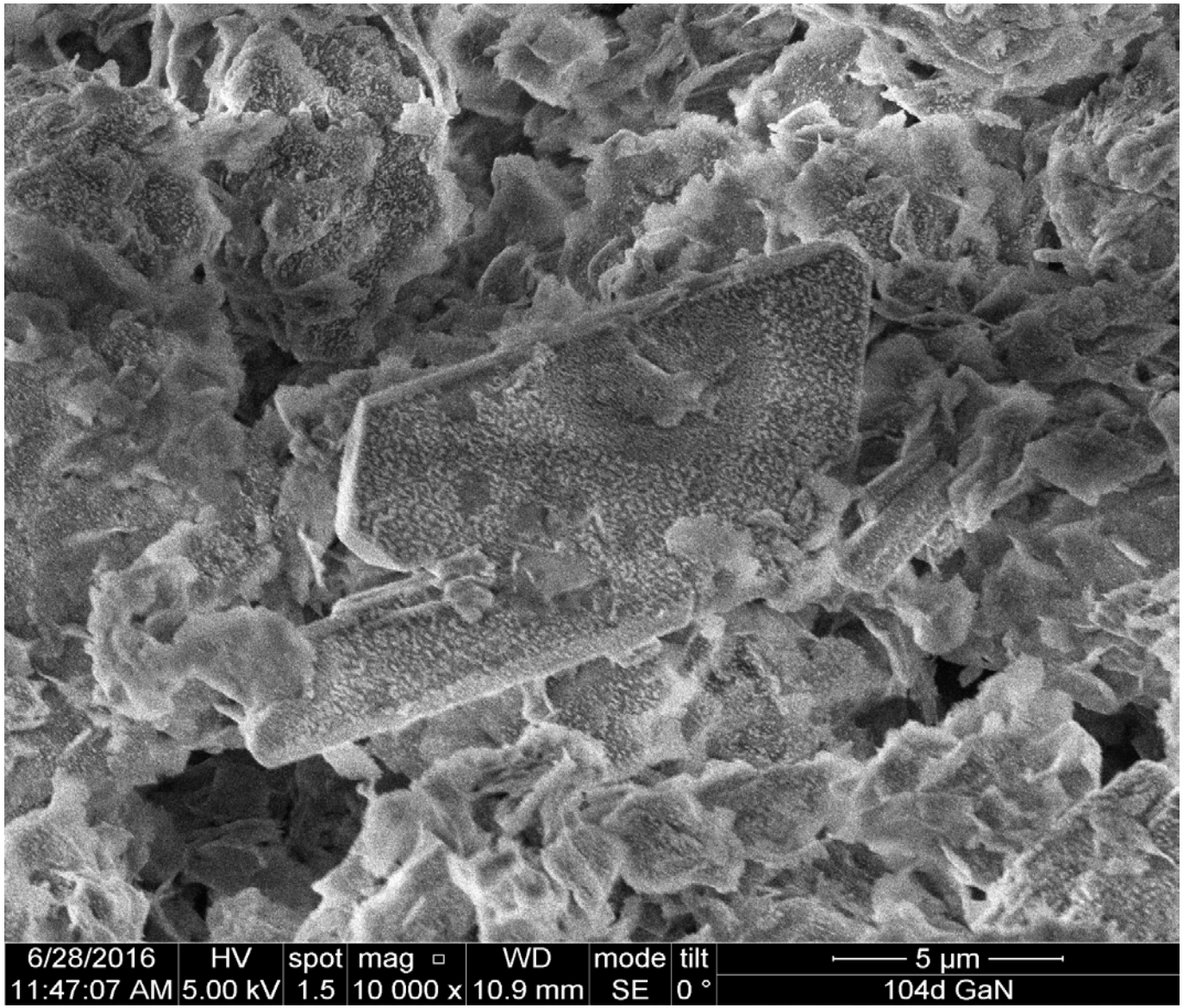

Figure E.2. Clinozoisite in sample DBS16 (Cs/Ca/NaCl brine)

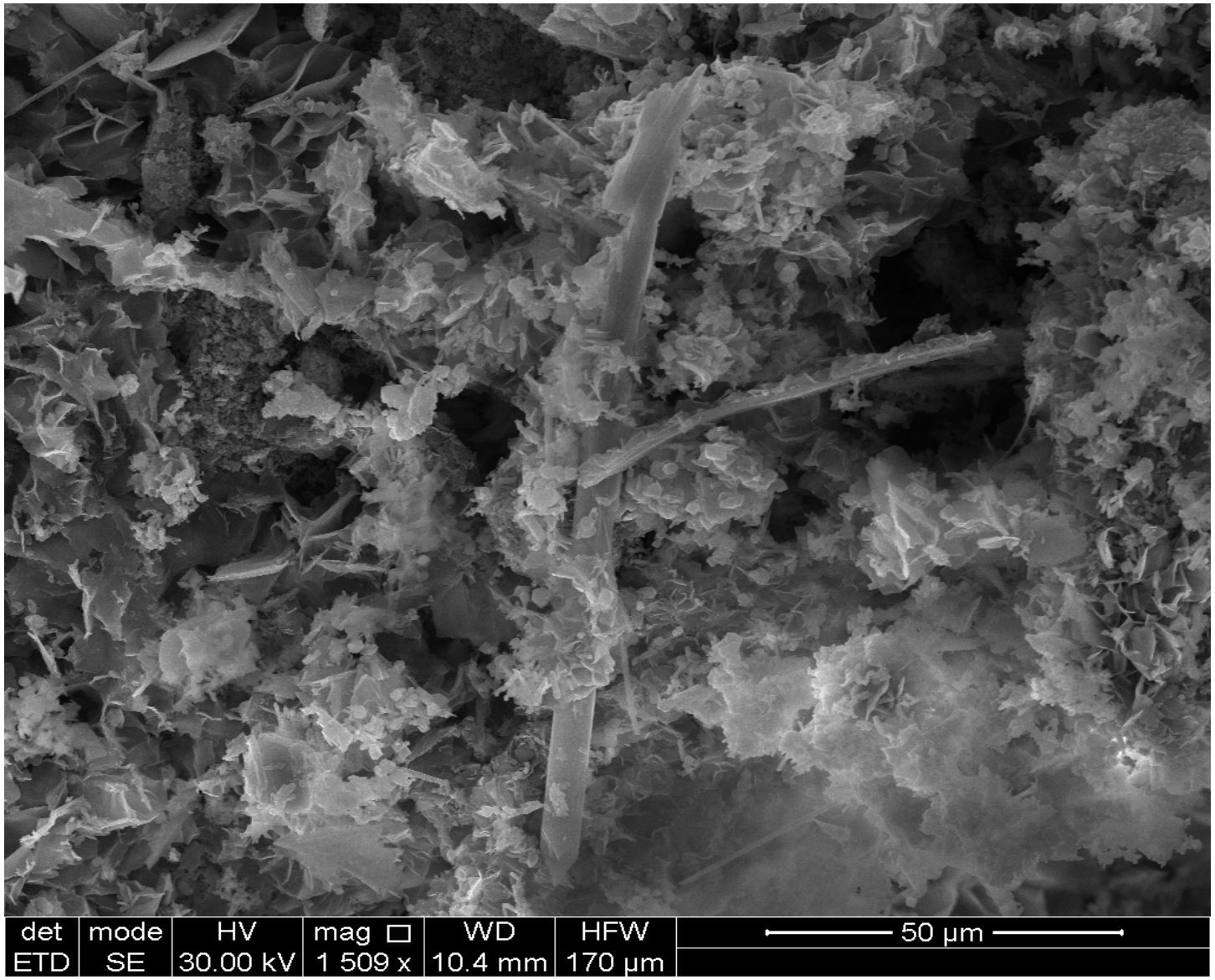

Figure E.3. Acicular ferrosilite in sample DBS11 (CaCl brine)

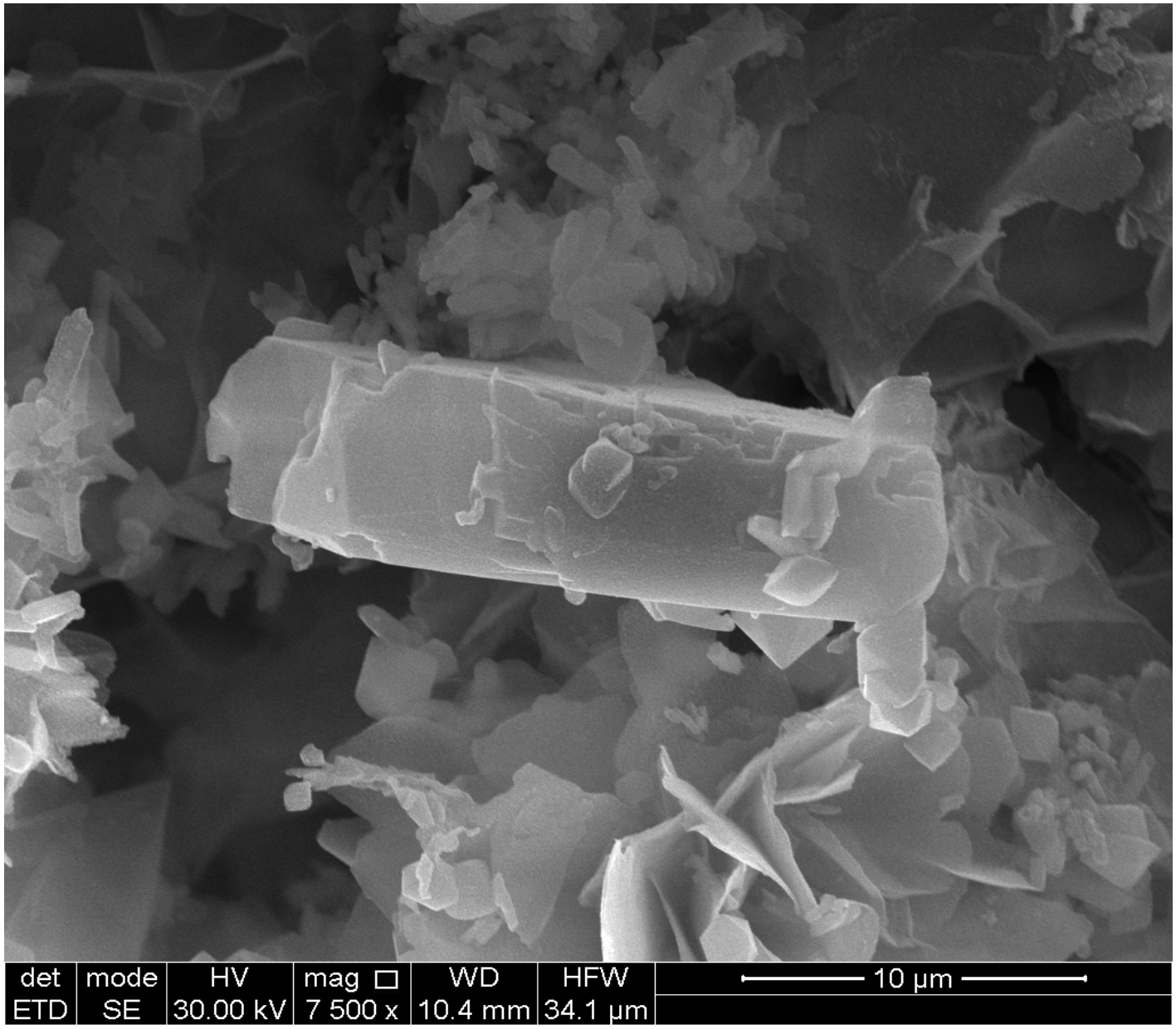

Figure E.4. Iron rich Amphibole in sample DBS11 (CaCl brine)

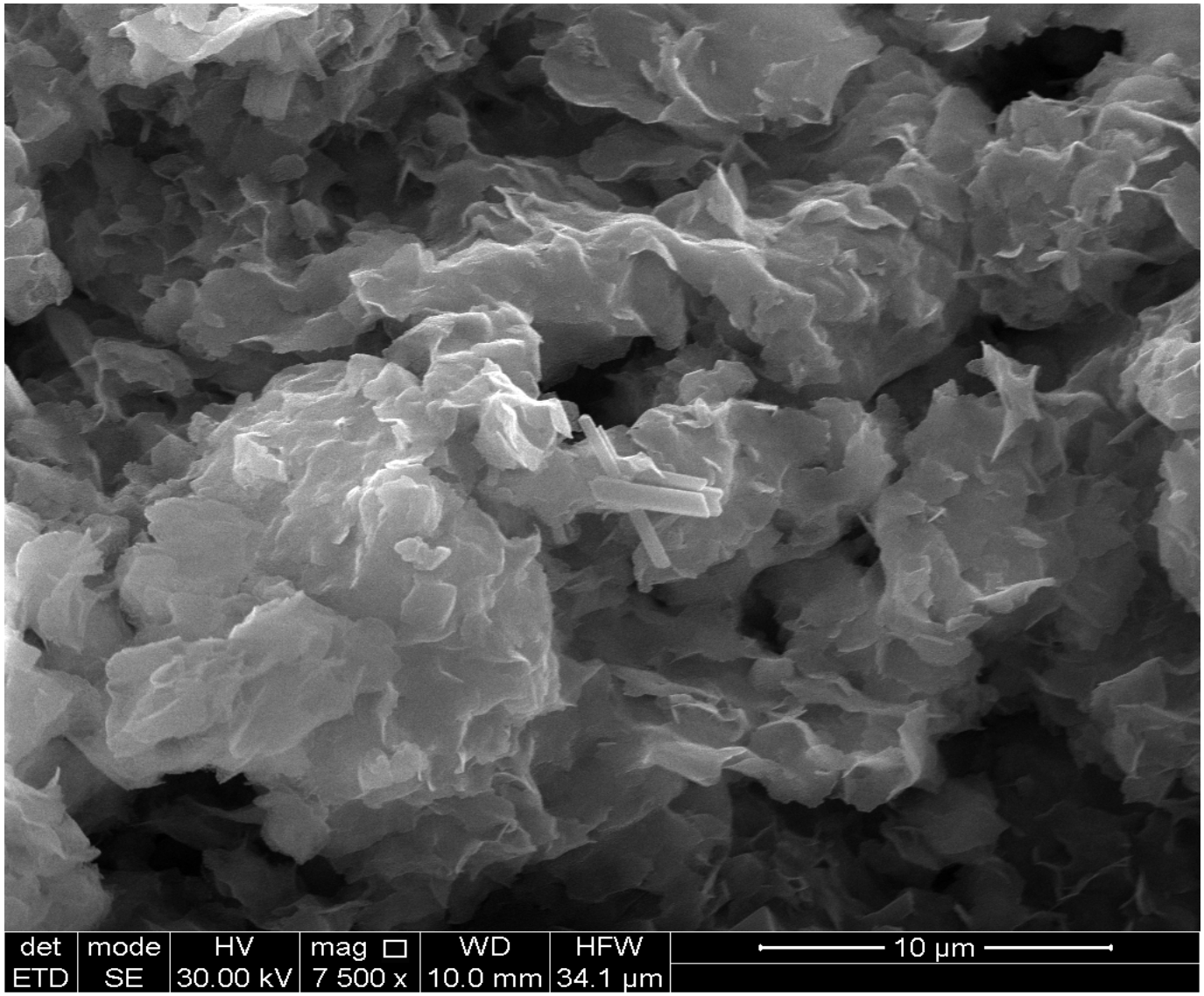

Figure E.5. Euhedral chlorite on relict smectite grain in sample DBS16 (Cs/Ca/NaCl brine)

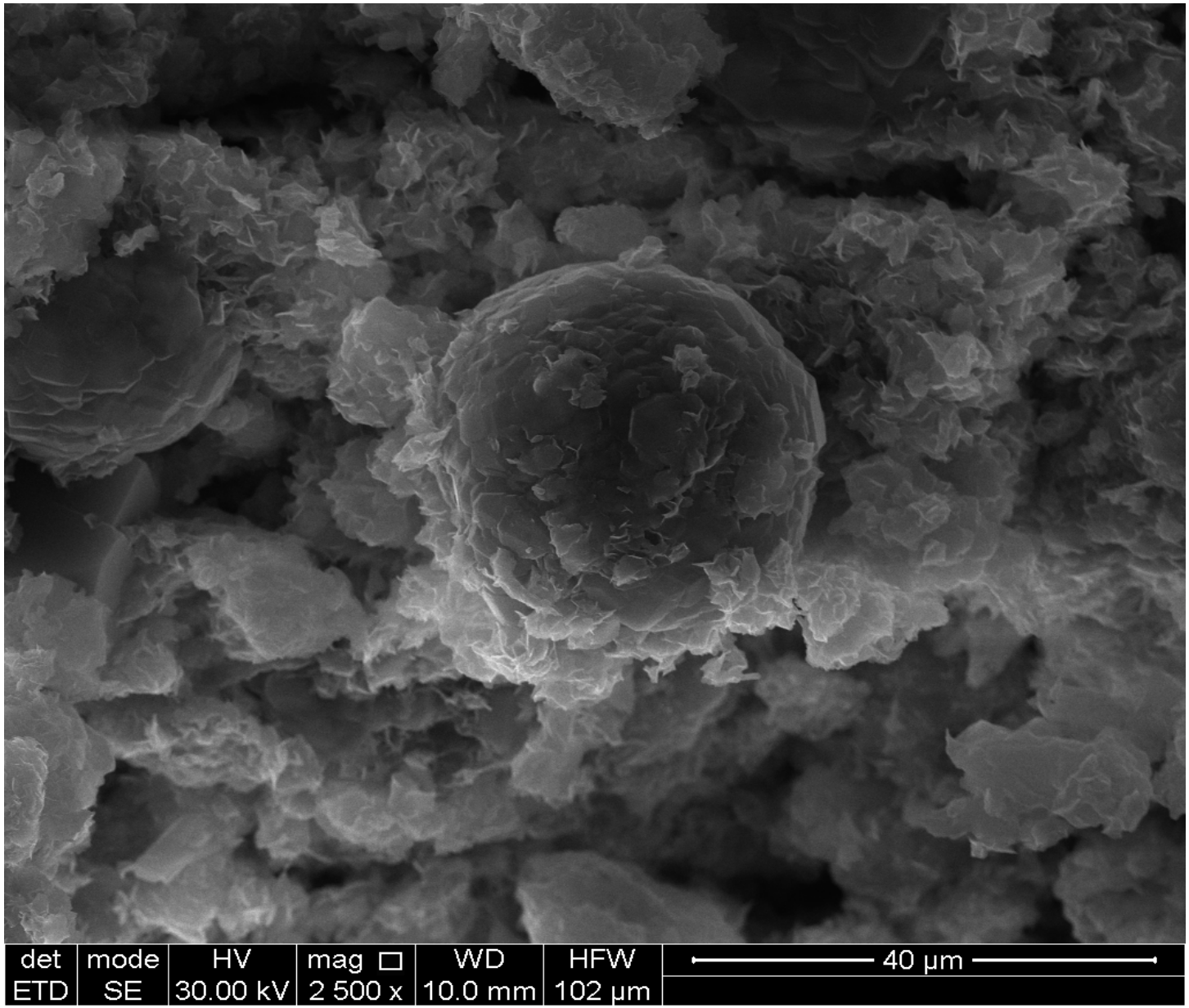

Figure E.6. Cs-rich analcime zeolite with relict smectite in sample DBS16 (Cs/Ca/NaCl brine)